The Plant Cell, Vol. 25: 499–516, February 2013, www.plantcell.org © 2013 American Society of Plant Biologists. All rights reserved.

Clathrin Light Chains Regulate Clathrin-Mediated Trafficking, Auxin Signaling, and Development in *Arabidopsis*[C][W][OA]

Chao Wang,[a] Xu Yan,[a,1] Qian Chen,[b,1] Nan Jiang,[a,1] Wei Fu,[a] Bojun Ma,[a] Jianzhong Liu,[a] Chuanyou Li,[b] Sebastian Y. Bednarek,[c] and Jianwei Pan[a,2]

[a] College of Chemistry and Life Sciences, Zhejiang Normal University, Zhejiang 321004, China
[b] State Key Laboratory of Plant Genomics, National Center for Plant Gene Research (Beijing), Institute of Genetics and Developmental Biology, Chinese Academy of Sciences, Beijing 100101, China
[c] Department of Biochemistry, University of Wisconsin, Madison, Wisconsin 53706

Plant clathrin-mediated membrane trafficking is involved in many developmental processes as well as in responses to environmental cues. Previous studies have shown that clathrin-mediated endocytosis of the plasma membrane (PM) auxin transporter PIN-FORMED1 is regulated by the extracellular auxin receptor AUXIN BINDING PROTEIN1 (ABP1). However, the mechanisms by which ABP1 and other factors regulate clathrin-mediated trafficking are poorly understood. Here, we applied a genetic strategy and time-resolved imaging to dissect the role of clathrin light chains (CLCs) and ABP1 in auxin regulation of clathrin-mediated trafficking in *Arabidopsis thaliana*. Auxin was found to differentially regulate the PM and *trans*-Golgi network/early endosome (TGN/EE) association of CLCs and heavy chains (CHCs) in an ABP1-dependent but TRANSPORT INHIBITOR RESPONSE1/AUXIN-BINDING F-BOX PROTEIN (TIR1/AFB)-independent manner. Loss of CLC2 and CLC3 affected CHC membrane association, decreased both internalization and intracellular trafficking of PM proteins, and impaired auxin-regulated endocytosis. Consistent with these results, basipetal auxin transport, auxin sensitivity and distribution, and root gravitropism were also found to be dramatically altered in *clc2 clc3* double mutants, resulting in pleiotropic defects in plant development. These results suggest that CLCs are key regulators in clathrin-mediated trafficking downstream of ABP1-mediated signaling and thus play a critical role in membrane trafficking from the TGN/EE and PM during plant development.

INTRODUCTION

Clathrin-mediated endocytosis (CME) is an evolutionally conserved endocytic pathway that plays a pivotal role in the regulation of protein abundance at the plasma membrane (PM) and/or the *trans*-Golgi network (TGN) during signaling events and retargeting or degradation of membrane proteins (Chen et al., 2011; McMahon and Boucrot, 2011). Clathrin is a triskelion-shaped complex consisting of three heavy chains (CHCs), which form the structural backbone of the clathrin lattice, and three light chains (CLCs) (Royle, 2006), which have been suggested in mammalian and yeast cells to regulate the formation of clathrin-coated vesicles (CCVs) (Ybe et al., 1998; Newpher et al., 2006; Royle, 2006; Mettlen et al., 2009). During CME, clathrin triskelia associate with the PM and polymerize to form clathrin-coated pits (CCPs) through their interaction with cargo proteins, the adaptor protein 2 complex (composed of α, β2, μ2, and σ2 subunits) and accessory adaptor proteins, such as clathrin assembly protein AP180 and Epsin (Royle, 2006). CCPs harboring cargoes initiate, invaginate, and eventually mature as CCVs through pinching off the PM.

In plants, clathrin-dependent membrane trafficking is critical for a number of developmental processes, including the determination of cell polarity (Dhonukshe et al., 2008; Mravec et al., 2011), cytokinesis (Kang et al., 2003; Van Damme et al., 2011), cell elongation (Zhao et al., 2010), embryogenesis (Kitakura et al., 2011), and gametogenesis (Backues et al., 2010). Plant CLCs and CHCs predominantly localize to the PM and TGN/early endosome (EE) compartments (Dhonukshe et al., 2007; Konopka et al., 2008; Robert et al., 2010; Ito et al., 2012), and CME regulates the internalization of critical PM proteins involved in hormone signaling (Geldner et al., 2007; Robert et al., 2010; Xu et al., 2010; Irani et al., 2012), defense or stress responses (Leborgne-Castel et al., 2008), and nutrient uptake (Barberon et al., 2011).

Auxin regulates many aspects of plant growth and development, such as root and shoot architecture, organ pattern formation, and vascular development, as well as responses to gravity and light (Leyser, 2011). The direction and flux of auxin within the plant and its intracellular accumulation are largely determined by the PM polar localization of auxin transporters, AUXIN RESISTANT1/LIKE AUX proteins (Swarup et al., 2005), ABC-type MULTIDRUG RESISTANCE/P-GLYCOPROTEINS (Geisler and Murphy, 2006; Blakeslee et al., 2007; Titapiwatanakun et al., 2009), and PIN-FORMED (PIN) proteins (Petrášek et al., 2006; Wisniewska et al., 2006). PIN-mediated auxin transport

[1] These authors contributed equally to this work.
[2] Address correspondence to jwpan@zjnu.cn.
The author responsible for distribution of materials integral to the findings presented in this article in accordance with the policy described in the Instructions for Authors (www.plantcell.org) is: Jianwei Pan (jwpan@zjnu.cn).
[C] Some figures in this article are displayed in color online but in black and white in the print edition.
[W] Online version contains Web-only data.
[OA] Open Access articles can be viewed online without a subscription.
www.plantcell.org/cgi/doi/10.1105/tpc.112.108373

plays a critical role in many developmental processes, including embryogenesis (Friml et al., 2003), organogenesis (Benková et al., 2003), vascular patterning (Gälweiler et al., 1998), and tropic growth (Ding et al., 2011; Wan et al., 2012). Consistent with a role for CME in PIN localization and function, recent analysis of loss-of-function *chc2* single mutants and transgenic lines expressing a dominant-negative form of *CHC1* (*HUB*) (Kitakura et al., 2011) has demonstrated that CHCs are required for the endocytosis and polar distribution of PIN proteins and play a critical role in plant developmental processes.

Auxin itself modulates the levels and distribution of PIN proteins through TRANSPORT INHIBITOR RESPONSE1/AUXIN-BINDING F-BOX PROTEIN (TIR1/AFB)-mediated regulation of PIN transcription and degradation (Sieberer et al., 2000; Vieten et al., 2005; Sauer et al., 2006a; Pan et al., 2009; Sun et al., 2011; Baster et al., 2012). In addition, auxin inhibits CME of PIN proteins via a rapid depletion of both CLCs and CHCs from the PM, which requires AUXIN BINDING PROTEIN1 (ABP1)-mediated auxin signaling (Robert et al., 2010; Sauer and Kleine-Vehn, 2011). However, little is known about molecular mechanisms underlying auxin/ABP1 regulation of PM- and TGN/EE-associated CLC or CHC levels and their function during membrane trafficking. Furthermore, the specific biochemical processes in which CLCs function during membrane trafficking are not well understood in any system, and their physiological and developmental roles in plants remain to be elucidated.

In this study, we used genetic and cytological approaches to dissect the roles of CLCs in clathrin-mediated trafficking and their function in plant growth and development. Our results demonstrate that CLCs regulate the membrane association of CHCs and auxin-dependent clathrin-mediated trafficking from the PM and TGN/EE downstream of ABP1-mediated signaling.

RESULTS

Auxin Differentially Regulates CLC and CHC Association with the Membranes

Bioinformatic analyses have identified two *CHC* and three *CLC* genes (*CLC1-3*) in the *Arabidopsis thaliana* genome (Holstein, 2002; Chen et al., 2011). CLC1-3 share ~55% amino acid identity with each other and ~30% identity with either mammalian CLCa or CLCb isoforms. Previous studies have demonstrated that CLC2-GFP (for green fluorescent protein) localizes to the TGN/EE and to dynamic PM-associated foci (Konopka et al., 2008; Ito et al., 2012), and upon auxin treatment, the levels of CLC2-GFP transiently disappear from the PM but remain constant at the TGN/EE (Robert et al., 2010).

To further assess the regulation and role of CLCs in auxin-dependent CME, we first reevaluated the effects of auxin on the localization and membrane association of CLCs. Five-day-old seedlings that express *CLC2-GFP* under control of its native promoter (*ProCLC2*:*CLC2-GFP*) (Konopka et al., 2008; Ito et al., 2012) were treated with exogenous auxin 2,4-dichlorophenoxyacetic acid (2,4-D; 10 μM) for different lengths of time and the levels of PM- and TGN/EE-associated CLC2-GFP were analyzed by confocal laser scanning microscopy (CLSM). As previously reported (Robert et al., 2010), the levels of PM-associated CLC2-GFP in root epidermal cells transiently decreased after treatment with auxin for 5 min and reappeared at the PM after 60 to 120 min (see Supplemental Figures 1C to 1F and 1M online). No significant changes in the levels of PM-associated CLC2-GFP were detected in the different time mock controls (see Supplemental Figures 1A, 1B, and 1M online). However, in contrast with the results of Robert et al. (2010), the association of CLC2-GFP with the TGN/EE paralleled the auxin-stimulated loss, followed by recovery of the PM pool of CLC2-GFP (see Supplemental Figures 1A to 1F and 1M online). Similarly, analyses of the subcellular distribution of endogenous CLC1 in wild-type root epidermal cells by immunofluorescence (IF) microscopy using affinity-purified anti-CLC1–specific antibodies (Figures 1A to 1F and 1M) and live-cell imaging of CLC1-GFP expressed under control of the constitutive cauliflower mosaic virus 35S promoter (see Supplemental Figures 1G to 1L and 1N online) showed that the PM and TGN/EE association of the CLC1 isoform was also regulated by exogenous auxin. Furthermore, the levels of PM- and TGN/EE-associated endogenous CLC1 (Figure 1) and the CLC1-GFP and CLC2-GFP fusion proteins (see Supplemental Figure 1 online) displayed similar kinetic profiles in terms of their transient loss after 5 to 30 min and subsequent recovery after 120 min in response to exogenous auxin treatment.

In yeast and animal cells, CLCs and CHCs assemble to form clathrin triskelia in vivo (McMahon and Boucrot, 2011). Therefore, we tested the effects of auxin on the levels of membrane-associated CHCs by IF microscopy using affinity-purified anti-CHC–specific antibodies. Surprisingly, in contrast with CLCs, the levels of PM- and TGN/EE-associated CHCs appeared to initially increase after auxin treatments for 5 and 30 min (Figures 1G to 1J). The intensity of the CHC signal at the PM and TGN/EE increased by ~50% relative to the mock controls (Figure 1N). However, after 60 min, the levels of PM- and TGN/EE-associated CHCs were found to significantly decrease in auxin-treated seedlings (Figures 1K, 1L, and 1N). Immunoblot analysis of microsomal membrane fractions from the whole wild-type seedlings in the presence or absence of exogenous auxin confirmed that the levels of membrane-associated CLC1 and CLC2 initially decreased, whereas CHC levels increased 30 min after 2,4-D addition relative to those in mock-treated seedlings (see Supplemental Figure 2A, lanes 1 and 2, online). Subsequently, the levels of membrane-associated CLC1 and CLC2 returned to wild-type levels, whereas CHC levels decreased 120 min after 2,4-D addition (see Supplemental Figure 2B, lanes 1 and 2, online), consistent with CLSM analysis of CLC and CHC subcellular localization in root epidermal cells (Figure 1; see Supplemental Figure 1 online). The differential effects of the auxin, 2,4-D on the levels of PM- and TGN/EE-associated CHCs and CLC1-GFP were shown to be coordinated within individual cells expressing endogenous CHCs and CLC1-GFP (see Supplemental Figure 3 online).

2,4-D is a synthetic auxin and we therefore examined the effects of natural and other synthetic auxin analogs on the PM and TGN/EE association of clathrin subunits. Similar to the effects of 2,4-D, naphthalene-1-acetic acid (1-NAA; 10 μM) and the natural auxin indole-3-acetic acid (IAA; 20 μM) were found to differentially affect the PM and TGN/EE association of CLC1 and CHCs (see Supplemental Figures 4A to 4N online). Conversely, a structural analog of 1-NAA, naphthalene-2-acetic acid (2-NAA; 20 μM), which has no biological auxin activity,

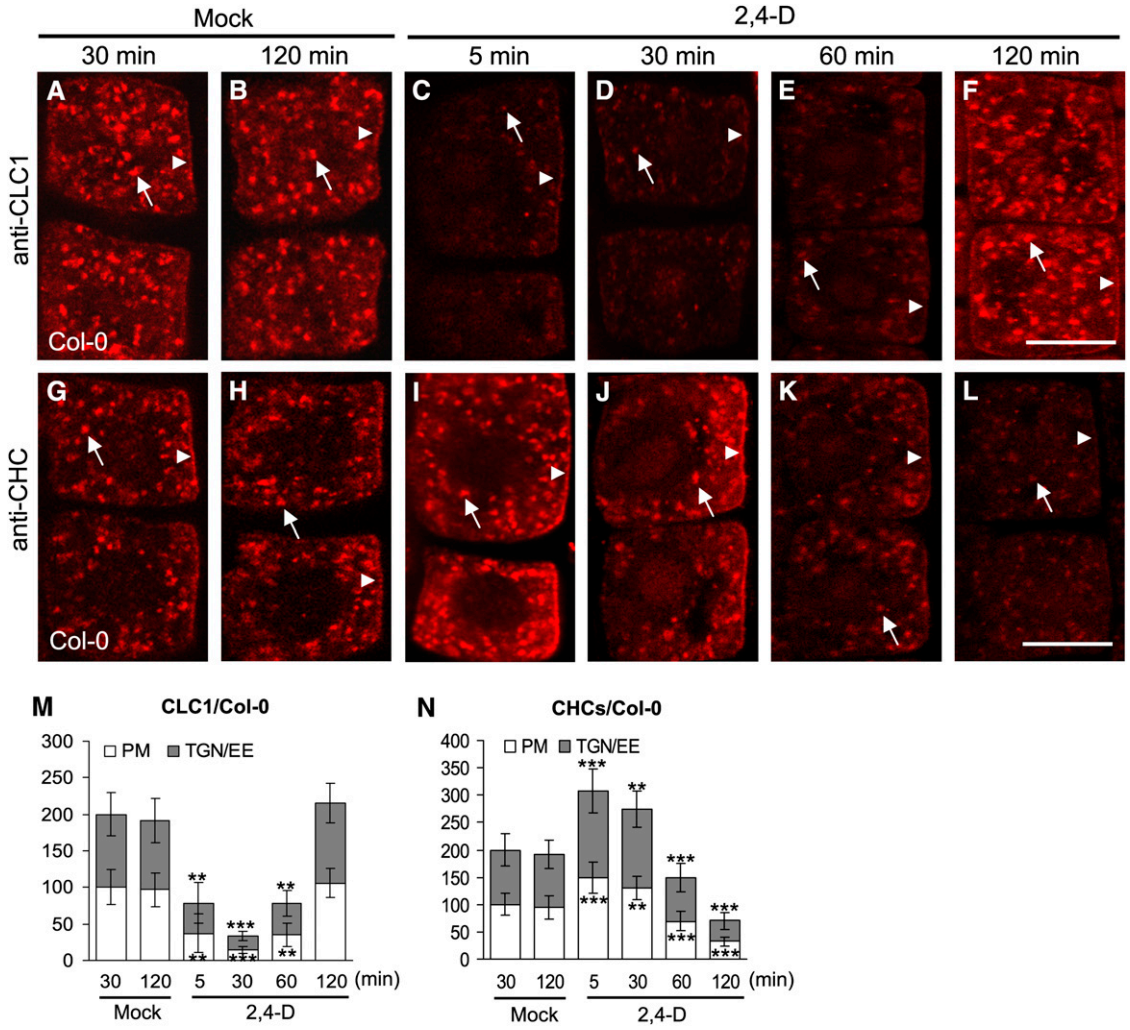

Figure 1. Kinetics of Auxin Effects on Membrane-Associated CLC1 and CHCs.

(A) to **(F)** Auxin effect on PM- and TGN/EE-associated CLC1 in the wild type.
(G) to **(L)** Auxin effect on PM- and TGN/EE-associated CHCs in the wild type.
(M) The relative intensity of CLC1 at the PM and TGN/EE (**[A]** to **[F]**).
(N) The relative intensity of CHCs at the PM and TGN/EE (**[G]** to **[L]**).
Different time lengths (5, 30, 60, and 120 min) after addition of 2,4-D (10 μM) or in the absence of exogenous auxin (mock controls) are indicated at the top of the figure. Arrows and arrowheads show TGN/EE- and PM-associated CLC1 or CHCs, respectively. Shown are means ± SD. Double and triple asterisks indicate $P < 0.001$ and 0.0001, respectively (Student's *t* test). Bars = 10 μm.

and 5-fluoroindole-3-acetic acid (5-F-IAA; 20 μM), which promotes auxin-dependent gene transcription but does not inhibit PIN1 internalization (Robert et al., 2010), had no affect on the subcellular distribution of CLC1-GFP and CHCs (see Supplemental Figures 4O to $4Z_3$ online). These data further support our finding that auxin differentially regulates membrane association of CLCs and CHCs in plants.

Effects of Cycloheximide and MG132 on CLC and CHC Association with Membranes

Based upon our analysis of the effects of 2,4-D on the PM- and TGN/EE-associated CLC1-GFP levels (see Supplemental Figure 1 online), which is expressed under the auxin-independent transcriptional control of the cauliflower mosaic virus 35S promoter (Liu et al., 1994) and the lack of any effect by 5-F-IAA (see Supplemental Figure 4 online), we hypothesized that the initial auxin-dependent changes in the CLC and CHC membrane association would be mediated through posttranscriptional processes. Indeed, using quantitative real-time RT-PCR analysis, we detected no significant differences between the levels of *CLCs* and *CHCs* mRNA in mock-treated versus 2,4-D–treated seedlings for 30 and 120 min (see Supplemental Figure 5A and Supplemental Table 1 online). Similarly, the effects of auxin on the initial changes in CLC and CHC association with the PM and TGN/EE were not blocked by cycloheximide (CHX; 50 μM),

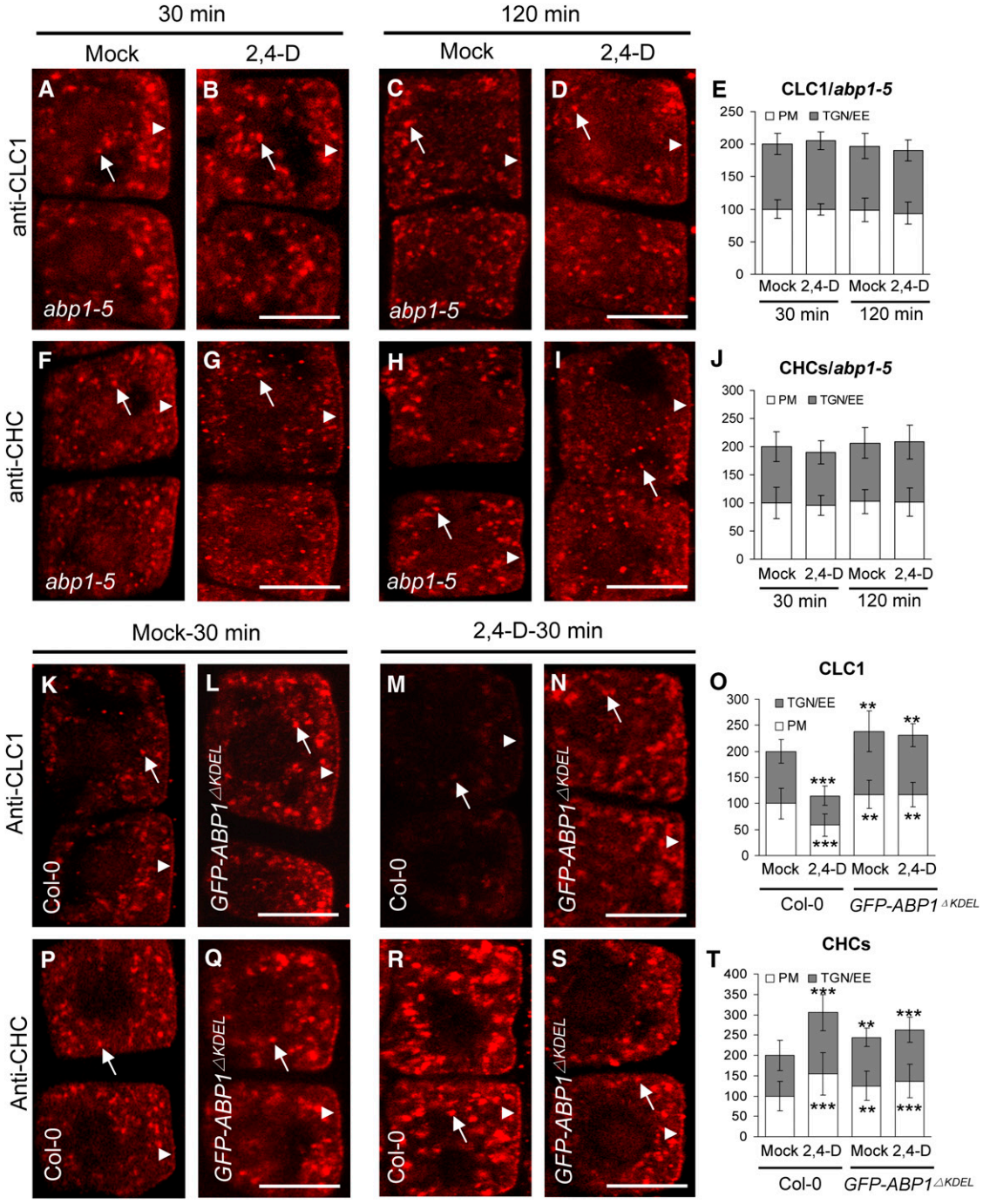

Figure 2. Differential Auxin Regulation of Membrane-Associated CLC1 and CHCs Is ABP1 Dependent.

(A) to **(J)** Impaired auxin regulation of the membrane association of CLC1 (**[A]** to **[E]**) and CHCs (**[F]** to **[J]**) in *abp1-5*. **(E)** and **(J)** show the relative intensities of CLC1 and CHCs at the PM and TGN/EE, respectively.

(K) to **(T)** ABP1 gain of function affects auxin regulation of the membrane association of CLC1 (**[K]** to **[O]**) and CHCs (**[P]** to **[T]**) in *GFP-ABP1*$^{\Delta KDEL}$ transgenic lines. **(O)** and **(T)** show the relative intensities of CLC1 and CHCs at the PM and TGN/EE, respectively.

Arrows and arrowheads show TGN/EE- and PM-associated CLC1 or CHCs, respectively. Shown are means ± SD. Double and triple asterisks indicate $P < 0.01$ and 0.0001, respectively (Student's *t* test). Bars = 10 μm.

a *de novo* protein synthesis inhibitor or MG132 (50 μM), an inhibitor of proteasome-mediated protein degradation as demonstrated by CLSM analysis of root epidermal cells (see Supplemental Figures 6A to 6N online), and by immunoblot analysis of membrane fractions from mock- and 2,4-D–treated seedlings for 30 min (see Supplemental Figure 2A, lanes 3 and 4, online). As shown by CLSM imaging, CHX or MG132 alone treatment for 30 min did not significantly affect the levels of PM- and TGN/EE-associated CLC1-GFP and CHCs (see Supplemental Figures 6G and 6N online).

However, de novo protein synthesis was required for the observed restoration (120 min), following the transient auxin-stimulated reduction, of membrane-associated CLC levels. As shown in Supplemental Figure 6 online, CHX, but not MG132, inhibited the reappearance of CLC1-GFP at the PM and TGN/EE in the presence of 2,4-D (see Supplemental Figures 6R to 6U online) and was restored to wild-type levels upon CHX washout (see Supplemental Figures 6S, inset, and 6U online). Similarly, immunoblot analysis showed that the levels of membrane-associated CLC1 and CLC2 were reduced in seedlings treated with CHX and 2,4-D but not with MG132 and 2,4-D, relative to seedlings treated solely with 2,4-D for 120 min (see Supplemental Figure 2B, lanes 2 to 4, online). Conversely, as shown by CLSM imaging and immunoblot analysis, MG132, but not CHX, inhibited the loss of PM- and TGN/EE-associated CHCs after 120-min treatments with 2,4-D (see Supplemental Figures $6Z_1$ to $6Z_3$ and 2B, lanes 3 and 4, online), suggesting that auxin-mediated loss of membrane-associated CHCs is dependent on proteasome-mediated protein degradation. As shown by CLSM imaging, CHX treatment, but not MG132 alone, for 120 min slightly but significantly decreased the levels of PM- and TGN/EE-associated CLC1-GFP and CHCs (see Supplemental Figures 6U and $6Z_3$ online).

Differential Auxin Regulation of CLC and CHC Membrane Association Is Dependent on ABP1 but Not TIR1/AFB Signaling

To determine whether the differential auxin-regulated PM and TGN/EE association of CLCs and CHCs is dependent upon ABP1 and/or E3 ubiquitin ligase $SCF^{TIR1/AFB}$, we examined the kinetics of auxin effects on CLC and CHC membrane localization in various auxin-signaling mutants by IF microscopy and immunoblot analysis. As in the wild type, auxin differentially regulated the PM and TGN/EE association of CLC1 and CHCs in *tir1 afb1*, *2*, *3* (see Supplemental Figures 7A to 7J online), a nuclear-localized auxin receptor quadruple mutant (Dharmasiri et al., 2005). Similar results were observed in *axr1-12*, a ubiquitin-activating enzyme E1 mutant (Leyser et al., 1993), and *axr6-3*, a SCF subunit CUL1 mutant (Quint et al., 2005) (see Supplemental Figures 7K to 7T online), suggesting that $SCF^{TIR1/AFB}$-mediated auxin signaling is not directly involved in the differential auxin regulation of CLC and CHC membrane association. As shown in Figure 2, the auxin-mediated transient depletion and increase in the membrane association of CLC1 and CHCs, respectively, were abolished in *abp1-5* mutants that contain an amino acid substitution (H94Y) in the ABP1 potential auxin binding site (Robert et al., 2010; Xu et al., 2010) and the supposed ABP1 gain-of-function *GFP-ABP1*$^{\Delta KDEL}$ transgenic lines (Robert et al., 2010). It is likely that the lack of KDEL, an endoplasmic reticulum C-terminal tetrapeptide retention signal, reduces auxin-signaling function of GFP-APB1$^{\Delta KDEL}$ through disrupting its subcellular localization. In the absence of exogenous auxin, the levels of PM- and TGN-associated CLC1 and CHCs were similar to the wild type in these auxin-signaling mutants examined (see Supplemental Figures 8A to 8E, 8G to 8K, 8M, and 8N online) with the exception that increased levels of membrane-associated CLC1 and CHCs were observed in *GFP-ABP1*$^{\Delta KDEL}$ transgenic lines, compared with wild-type mock controls (Figures 2O and 2T), consistent with the model that in the absence of auxin, ABP1 plays a positive role in endocytosis (Robert et al., 2010) and potentially clathrin-dependent trafficking from the TGN/EE.

In addition, immunoblot analysis further confirmed that auxin differentially affected the levels of membrane-associated CLC2 and CHCs in *axr1-12* and *axr6-3* mutant seedling membrane fractions similarly to in the wild type, whereas there was no observed transient decrease of CLC2 (30 min) or loss of CHCs (120 min) in auxin-treated *abp1-5* mutants (see Supplemental Figures 2C and 2D online). Moreover, in the absence of exogenous auxin, the levels of membrane-associated CLC2, CLC1, and CHCs in *axr-12*, *axr6-3*, and *abp1-5* mutants were similar to those in the wild type (see Supplemental Figures 2E and 2F online). Together, these results suggest that the differential auxin regulation of CLC and CHC membrane association is dependent on ABP1-mediated, but not TIR1/AFB-mediated, auxin signaling.

clc Mutants Display Pleiotropic Developmental Defects

To explore the molecular mechanisms underlying the observed differential effects of auxin on the membrane association of CLCs and CHCs, we identified mutant lines containing T-DNA insertions in the three genes encoding CLC1, 2, and 3 (see Supplemental Figures 9A to 9C online). Homozygous *clc1-1* mutants could not be obtained as *clc1-1* pollen was not viable, and their further characterization will be reported elsewhere.

In contrast with *clc1* mutants, single homozygous *clc2-1* and *clc3-1* as well as double homozygous *clc2-1 clc3-1* mutant seedlings were found to be viable. However, these mutants displayed numerous developmental defects. As shown in Figures 3A to 3C, 5-d-old *clc2-1* and *clc3-1* seedlings have shorter primary roots and longer hypocotyls relative to the wild type. This phenotype was significantly enhanced in the *clc2-1 clc3-1* double mutant seedlings relative to either their single mutants or the wild type, suggesting that CLC2 and CLC3 are functionally redundant. In addition, 3-week-old double mutants exhibited up-curled leaves with longer petioles and fewer trichomes relative to the wild type (Figures 3D to 3H), phenotypes that were not observed in the single mutant plants. In the flowering double mutant plants, the inflorescence stems were more highly branched and prostrate with shorter siliques than the wild type (Figures 3I to 3K). In addition, root hair polarity (Grebe et al., 2002) and the initiation of lateral root primordia (LRP) (Benková et al., 2003) were altered in the double mutants (Figures 3L and 3M; see Supplemental Figures 9D to 9F online). These phenotypes are characteristic of defects in auxin signaling and/or transport and indicate that

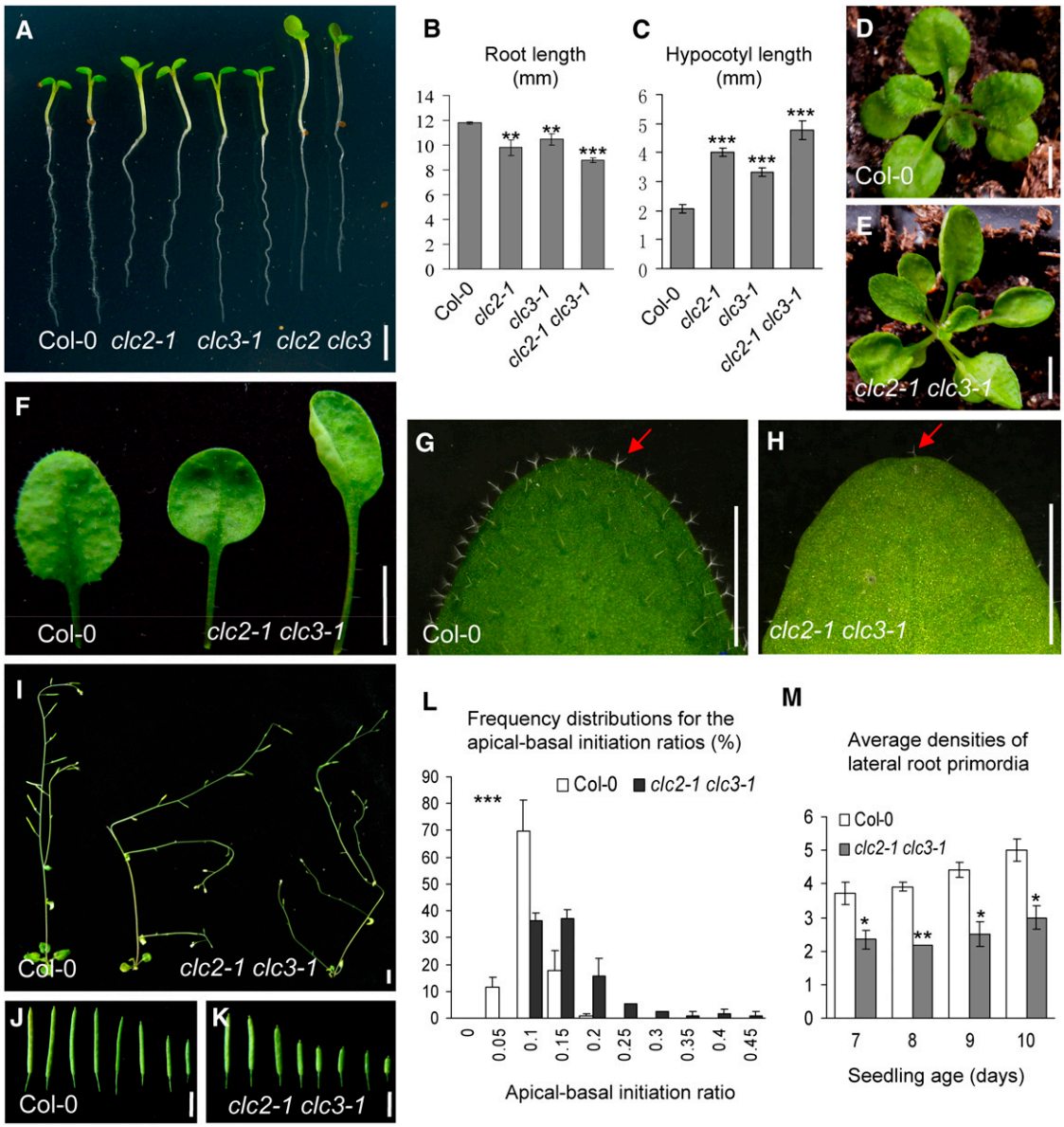

Figure 3. Developmental Defects in *clc2-1 clc3-1*.

(A) to **(C)** Five-day-old vertically grown seedlings in the wild type and *clc* single and double mutants were transferred on to the new plates for imaging **(A)**, and the lengths of roots **(B)** and hypocotyls **(C)** was measured.
(D) to **(H)** Phenotypes of 3-week-old seedlings in the wild type **(D)** and *clc2-1 clc3-1* **(E)**.
(F) Leaf phenotypes including petioles.
(G) and **(H)** Trichomes indicated by arrows.
(I) to **(K)** Five-week-old seedlings and siliques of the wild type and *clc2-1 clc3-1*.
(L) Frequency distributions for the apical-basal initiation ratios of root trichoblast cells. Triple asterisks ($P < 0.001$) indicate the significance level for independence of distributions between the wild type and *clc2-1 clc3-1*.
(M) Average densities of LRPs in the wild type and *clc2-1 clc3-1*.
Detailed information for **(L)** and **(M)** is shown in Methods and Supplemental Figures 9D to 9F online. Bars = 2 mm in **(A)** and 5 mm in **(D)** to **(K)**. Shown are means ± SD. Single, double, and triple asterisks (**[B]**, **[C]**, and **[M]**) indicate $P < 0.05$, 0.01, and 0.0001, respectively (Student's *t* test; compared with the corresponding wild-type control).
[See online article for color version of this figure.]

the loss of CLC2 and CLC3 causes auxin-related, pleiotropic developmental defects.

To confirm that these developmental defects are specific to the T-DNA insertional mutations in *clc2-1* and *clc3-1*, we generated transgenic homozygous *clc2 clc3* double mutants that expressed rescue constructs for both CLC2 and CLC3 under control of their native promoters (*clc2 clc3*::*CLC2 CLC3*). As shown in Supplemental Figures 9G to 9I online, the *clc2 clc3*::*CLC2 CLC3* rescue lines displayed phenotypically wild-type growth and development with no discernible auxin-related defects.

CLCs Regulate Clathrin-Mediated Trafficking and CHC Membrane Association

To determine whether CLCs regulate general CME and/or endocytic trafficking, we first analyzed the internalization in the *clc2 clc3* double mutants of GFP fusions of two PM marker proteins that have distinct functions, the auxin efflux transporter PIN2 (PIN2-GFP; Xu and Scheres, 2005) and the rare cold-inducible protein RCI2A (RCI2-GFP; Cutler et al., 2000), which may function in response to abiotic stress (Medina et al., 2007). Previous studies have demonstrated that the internalization of FM4-64 (N-(3-triethylammoniumpropyl]-4[6-(4-(diethylamino)phenyl) hexatrienyl]pyridinium dibromide), a lipophilic styryl dye and PIN2 is dependent on CME (Dhonukshe et al., 2007) and is regulated by auxin/ABP1 (Paciorek et al., 2005; Robert et al., 2010). To confirm that internalization of PM-localized RCI2A-GFP is also clathrin dependent, we examined the effects of tyrphostin A23, an inhibitor of CME, and its structural analog, tyrphostin A51, which does not affect CME (Banbury et al., 2003; Dhonukshe et al., 2007; Konopka et al., 2008), on RCI2A-GFP internalization, in the presence of the vesicle trafficking inhibitor Brefeldin A (BFA; 50 μM), which induces the clustering of late secretory pathway compartments into BFA bodies (Geldner et al., 2001, 2003; Lam et al., 2009) and thereby inhibits the recycling and/or transport of endocytosed proteins to the PM and/or vacuoles. As shown in Supplemental Figures 10A to 10D online, tyrphostin A23 (30 μM) was found to significantly inhibit the intracellular accumulation of RCI2A-GFP in BFA bodies, whereas tyrphostin A51 (30 μM) did not affect RCI2A-GFP internalization. Together, these results indicate that PM-localized RCI2A-GFP is internalized via CME.

To examine whether CME is affected in *clc2 clc3* double mutants, we assessed the accumulation of PIN2-GFP and RCI2A-GFP in BFA bodies and the internalization of FM4-64. We found that the densities of PIN2-GFP– and RCI2A-GFP–labeled BFA bodies (15-min BFA treatment; Figures 4B and 4D; see Supplemental Figures 10F and 10H online) and levels of internalized FM4-64 after 30 min (see Supplemental Figures 11A to 11C online) in the double mutants were significantly lower than observed in wild-type cells, indicating impaired CME of PM proteins in the double mutants. However, no significant difference in the densities of PIN2-GFP– and RCI2A-GFP–labeled BFA bodies was detected between the wild type and the double mutants after BFA treatment for 60 min (Figures 4C and 4D; see Supplemental Figures 10G and 10H online). One potential reason for the difference between the number of GFP-labeled BFA bodies at the early and later time points is that the inhibition of internalization by the loss of CLC2 and CLC3 is not complete in the double mutants. Due to the observed reduction in PM protein internalization at early time points, we expected that the levels of PIN2-GFP at the PM would be elevated in the *clc2 clc3* double mutant root cells compared with the wild-type. Indeed, quantitative image analysis of seedling roots, treated with CHX to block the synthesis of new PIN2-GFP, showed that the PM levels of PIN2-GFP were higher in the double mutants than in the wild type in the absence of exogenous auxin (see Supplemental Figures 11D to 11F online). Together, these results suggest that internalization of PM proteins is impaired in the *clc2 clc3* double mutants.

Following internalization, PM proteins may be transported to vacuoles for degradation or be recycled back to the PM (Lam et al., 2007; Kleine-Vehn et al., 2008; Laxmi et al., 2008). Previous studies in plants have shown that the accumulation of internalized GFP-fused PM proteins in vacuoles can be visualized in light-grown seedlings following their incubation in the dark (Kleine-Vehn et al., 2008; Laxmi et al., 2008). The vacuolar accumulation of PIN2-GFP and RCI2A-GFP was significantly reduced in the *clc2-1 clc3-1* double mutants relative to the wild type after 2- or 4-h dark treatments (Figures 4E to 4H; see Supplemental Figures 10I to 10L online). To examine whether the recycling of internalized PIN2-GFP and RCI2A-GFP to the PM is also affected in the double mutants, we monitored, as previously described (Geldner et al., 2001, 2003), the loss of internalized PIN2-GFP and RCI2A-GFP from BFA bodies following BFA removal in the presence of CHX. As expected, the recycling back to the PM of internalized PIN2-GFP and RCI2A-GFP was slower in the double mutants than in the wild type (Figures 4I to 4U; see Supplemental Figures 10M to 10Y online).

To address the mechanism of the impaired internalization and intracellular trafficking of PM proteins observed in the *clc2 clc3* double mutants, we examined whether the loss of CLC2 and CLC3 affected the levels of PM- and TGN/EE-associated CLC1 and CHCs in the absence of exogenous auxin. As expected, the levels of PM- and TGN/EE-associated CHCs but not CLC1 were significantly reduced in the *clc2-1 clc3-1* mutant cells relative to wild-type cells (see Supplemental Figures 8F and 8L to 8N online), which was further supported by immunoblot analysis (see Supplemental Figure 2F online). Taken together, these results suggest that CLCs are required for the association of CHCs with the PM and TGN/EE necessary for clathrin-mediated trafficking.

CLC-Mediated Auxin Regulation of CHC Membrane Abundance

Next, we examined whether CLC2 and CLC3 are required for the observed differential auxin regulation of membrane-associated CLC1 and CHC levels. Similar to the wild type (Figures 1A to 1F), CLC1 was rapidly and transiently depleted from the PM and TGN/EE upon treatment of the *clc2-1 clc3-1* double mutants with exogenous auxin (Figures 5A to 5E), indicating that CLC2 and CLC3 are not required for auxin regulation of CLC1 membrane association. However, in contrast with the wild-type (Figures 1G to 1L), CHC levels at the PM and TGN/EE were not significantly affected in the auxin-treated *clc2-1 clc3-1* mutant seedlings (Figures 5F to 5J), which was supported by immunoblot

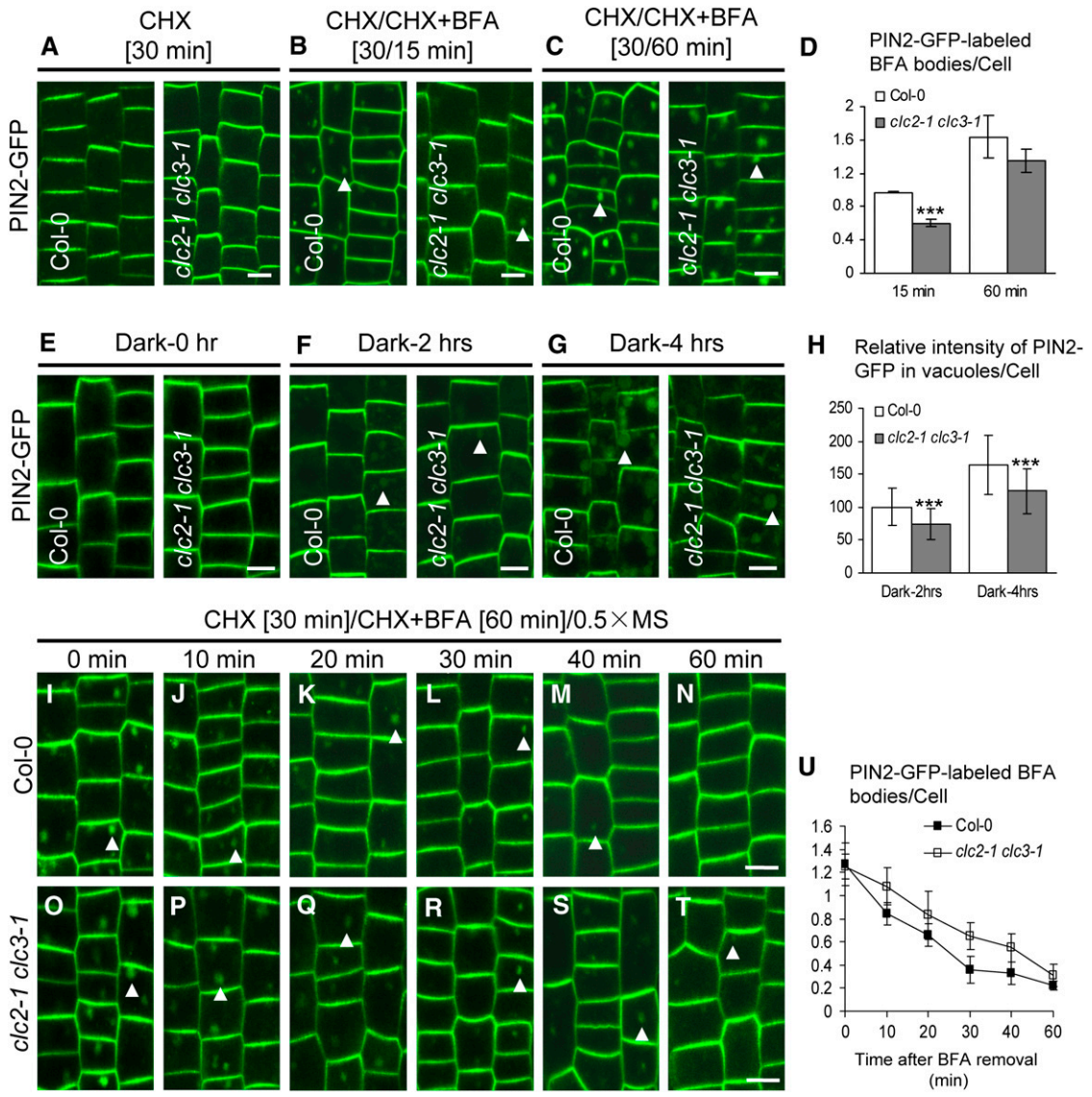

Figure 4. Impaired Trafficking of PIN2-GFP in *clc2-1 clc3-1*.

(A) to **(D)** BFA-induced internalization of PIN2-GFP in the wild type and *clc2-1 clc3-1*.
(A) CHX treatments for 30 min.
(B) and **(C)** CHX pretreatments for 30 min followed by washout with CHX and BFA for 15 min **(B)** and 60 min **(C)**.
(D) The average number of PIN2-GFP–labeled BFA bodies (**[B]** and **[C]**).
(E) to **(H)** Visualization of vacuolar accumulation of PIN2-GFP in dark-treated seedlings of the wild type and *clc2-1 clc3-1*.
(E) Dark treatments for 0 h.
(F) Dark treatments for 2 h.
(G) Dark treatments for 4 h.
(H) The average relative intensity of PIN2-GFP in vacuoles for each cell (**[F]** and **[G]**).
(I) to **(U)** Endocytic recycling of PIN2-GFP in the wild type and *clc2-1 clc3-1*. The seedlings were pretreated with CHX for 30 min, followed by washout with CHX and BFA for 60 min, and finally by washout with 0.5× MS liquid media for different lengths of time (0, 10, 20, 30, 40, and 60 min) in the wild type (**[I]** to **[N]**) and *clc2-1 clc3-1* (**[O]** to **[T]**) before CLSM imaging.
(U) The average number of PIN2-GFP–labeled BFA bodies after BFA removal in the wild type and *clc2-1 clc3-1*.
Arrowheads show PIN2-GFP–labeled BFA bodies or vacuoles. Bars = 10 μm. Shown are means ± SD. Triple asterisks indicate $P < 0.001$ **(D)** or 0.0001 **(H)**, respectively (Student's *t* test).
[See online article for color version of this figure.]

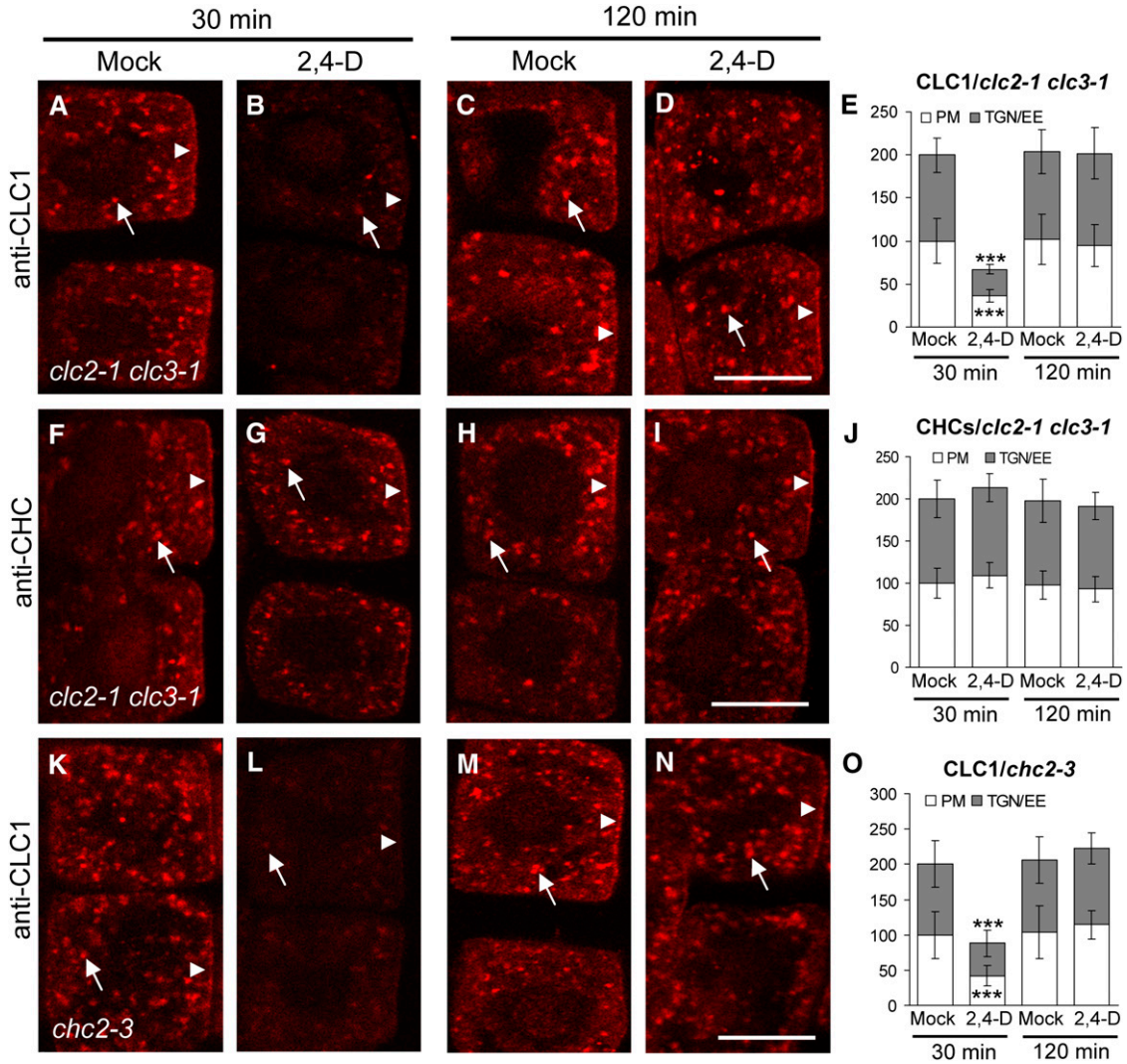

Figure 5. IF Analysis of Auxin and CLC2/3 Regulation of CHC Membrane Abundance.

(A) to **(J)** Auxin effects on PM- and TGN/EE-associated CLC1 (**[A]** to **[E]**) and CHCs (**[F]** to **[J]**) in *clc2-1 clc3-1*.
(K) to **(O)** Auxin effects on PM- and TGN/EE-associated CLC1 in *chc2-3*.
(E), **(J)**, and **(O)** The relative intensities of PM- and TGN/EE-associated CLC1 (**[E]** and **[O]**) and CHCs **(J)**.
Arrows and arrowheads show TGN/EE- and PM-associated CLC1 or CHCs, respectively. Bars = 10 μm. Shown are means ± SD. Triple asterisks indicate $P < 0.0001$, respectively (Student's *t* test).

analysis of CHC levels in membrane fractions prepared from the *clc2 clc3* mutant seedlings in the presence or absence of exogenous 2,4-D (see Supplemental Figure 2D, bottom panels, online). Furthermore, the qRT-PCR analysis showed that the levels of *CHC1/2* mRNA expression in the *clc2-1 clc3-1* mutant seedlings were similar to those in the wild type with or without the application of exogenous auxin (see Supplemental Figure 5 online). These results suggest that CLC2 and CLC3 mediate auxin regulation of CHC membrane abundance.

To address the reciprocal question, whether CHCs are essential for auxin regulation of membrane-associated CLC levels, we examined the auxin effects on CLC membrane abundance in *chc2* single mutants, which show significant phenotypic alterations in growth and development (Kitakura et al., 2011). In the *chc2* mutants (Figures 5K to 5O), auxin was found to regulate the levels of PM- and TGN/EE-associated CLC1 in the same manner as in the wild type (Figure 1) as well as in *clc2-1 clc3-1* (Figures 5A to 5E), indicating that CHC2 is not required for auxin regulation of CLC1 membrane abundance.

CLCs Are Essential for Auxin Inhibition of CME

As previously described, auxin inhibits the endocytosis of PIN proteins (Paciorek et al., 2005; Pan et al., 2009; Robert et al. 2010) as well as other PM-localized proteins, including RCI2A-GFP (see Supplemental Figure 12 online). To address the role of

CLCs in auxin inhibition of PM protein internalization, we analyzed the uptake of PIN2-GFP and endogenous PIN2 by live-cell and IF microscopy using affinity-purified anti-PIN2–specific antibodies, respectively, in the *clc2 clc3* double mutants treated with or without auxin. In the absence of exogenous auxin, the PM polar localization of PIN2-GFP and PIN2 was indistinguishable between the wild type and the double mutants (Figures 6A and 6F), indicating that CLC2 and CLC3 are not essential for the establishment and maintenance of PIN2 polarity in the root epidermal cells. BFA treatments, in the presence or absence of CHX, showed no significant difference in the number of PIN2-GFP– or PIN2-labeled BFA bodies was observed between the wild type and the double mutants (Figures 6B, 6E, 6G, and 6I), consistent with the previous observation (Figures 4C and 4D). Interestingly, in the presence of 10 μM 2,4-D (or 20 μM IAA), the number of PIN2-GFP– or PIN2-labeled BFA bodies in the double mutants was significantly higher than that in the wild type (Figures 6C to 6E, 6H, and 6I), reflecting that loss of CLC2 and CLC3 reduces the auxin inhibitory effect on PIN2 endocytosis. By contrast, auxin-mediated inhibition of PIN2 endocytosis was restored to the wild-type levels in the *clc2 clc3*::*CLC2 CLC3* rescue lines (Figures 6F to 6I). In the absence of BFA but in the presence of CHX, auxin effectively promoted an elevation in the levels of PM-associated PIN2-GFP in the wild type but not in the double mutants (see Supplemental Figures 11D to 11F online). These results demonstrate that CLC2 and CLC3 are essential for auxin regulation of PIN2 endocytosis.

To rule out the possibility that PIN2-GFP accumulation in BFA bodies in the auxin-treated *clc2 clc3* double mutant seedlings is due to the inhibitory effect of high BFA levels (50 μM) on the PIN2-GFP degradation, low BFA concentrations (25 μM) were used to examine internalization of PM-localized proteins. Indeed, auxin did not efficiently block internalization of PIN2-GFP, PIN1-GFP (Heisler et al., 2005), PIN3-GFP (Blilou et al., 2005), PIN7-GFP (Blilou et al., 2005), and RCI2A-GFP in the double mutants in the presence of 25 μM BFA and CHX (see Supplemental Figure 13 online). Together, these results suggest that CLCs are essential for auxin fine regulation of CME.

Defects in Auxin Sensitivity, Auxin Transport, and Gravitropism in *clc2 clc3* Mutants

Primary root growth of the heterozygous *abp1/ABP1* insertional mutants is resistant to exogenously applied auxin (Effendi et al., 2011), indicating that impairment of ABP1-mediated auxin signaling decreases auxin sensitivity. Our hypothesis based on the data presented above (Figures 1, 2, 5, and 6; see Supplemental Figures 2 and 7 online) is that CLC2 and CLC3 likely function in ABP1-mediated auxin signaling. To test this, we examined whether *clc2-1 clc3-1* double mutant root growth would be similarly resistant to exogenous auxin as observed for *abp1/ABP1* roots. Indeed, the double mutant root growth was significantly more resistant to 2,4-D at the concentrations of 0.05 and 0.1 μM relative to the wild-type roots ($P < 0.01$; Student's *t* test) (Figure 7A).

The growth of plant roots in response to gravity is finely and rapidly tuned via basipetal auxin transport that leads to an asymmetric distribution of auxin across the root tip (Rashotte et al., 2000; Abas et al., 2006), and PIN2 plays a pivotal role in this process (Shin et al., 2005; Abas et al., 2006). Thus, we predicted that altered PIN2 trafficking in the *clc2 clc3* double mutants (Figures 4 and 6) would affect PIN2-mediated basipetal auxin transport. We thus measured the root basipetal auxin transport in the wild type and the double mutants. As shown in Figure 7B, the root basipetal transport of tritium-labeled IAA (^{3}H-IAA) was increased by ~35% in the double mutants relative to that in the wild type, suggesting that CLCs play a inhibitory role in the PIN2-mediated basipetal auxin transport in planta.

As root basipetal auxin transport is critical for gravitropism (Rashotte et al., 2000), we next examined whether root gravitropic responses and auxin asymmetric distribution were altered in the double mutants. As expected, the roots of the *clc2-1 clc3-1* double mutant seedlings were defective in the gravitropic response (Figure 7C). In addition, expression of *DR5*:*GFP*, a reporter for auxin distribution (Benková et al., 2003), was found to be altered in the gravistimulated *clc2-1 clc3-1* roots. In contrast with the asymmetric distribution of *DR5*:*GFP* expression in gravistimulated wild-type roots, the *clc2-1 clc3-1* double mutant roots showed impaired auxin redistribution (Figures 7D to 7G). Together, our data demonstrate that CLC2 and CLC3 participate in the root gravitropism through the regulation of PIN2-mediated basipetal auxin transport and auxin asymmetric distribution.

DISCUSSION

Mechanisms of Differential Auxin Regulation of CLCs and CHCs

Clathrin-dependent membrane trafficking is essential for many aspects of plant growth and development (Holstein, 2002; Robert et al., 2010; Xu et al., 2010; Chen et al., 2011; Sauer and Kleine-Vehn, 2011). In contrast with yeast and animal cells (McMahon and Boucrot, 2011), however, the evolutionarily conserved as well as plant-specific mechanisms that regulate the formation and trafficking of CCVs are not well understood. Recent studies have demonstrated that auxin transport and signaling are highly dependent on CME for the PM polar localization of auxin efflux transporters, PINs, and that CME of PINs is itself regulated by auxin and ABP1 (Robert et al., 2010; Xu et al., 2010). Our time-resolved analysis of auxin effects on clathrin-mediated trafficking has both confirmed that ABP1 regulates CME in an auxin-dependent manner and provided further mechanistic insight into clathrin-mediated trafficking in plant cells. Specifically, our findings show that auxin promotes the differential association of CLCs and CHCs with the PM and TGN/EE. Interestingly, exogenous auxin was found to transiently enhance the levels of membrane-associated CHCs, while the levels of membrane-associated CLCs and the internalization of PIN and other PM proteins decreased (Figures 1 and 6; see Supplemental Figures 1 to 3 and 13 online). By contrast, however, the loss-of-function *clc2 clc3* mutants showed overall reduced levels of PM- and TGN/EE-associated CHCs relative to the wild type (see Supplemental Figures 2 and 8 online). How can we resolve these seemingly contradictory observations?

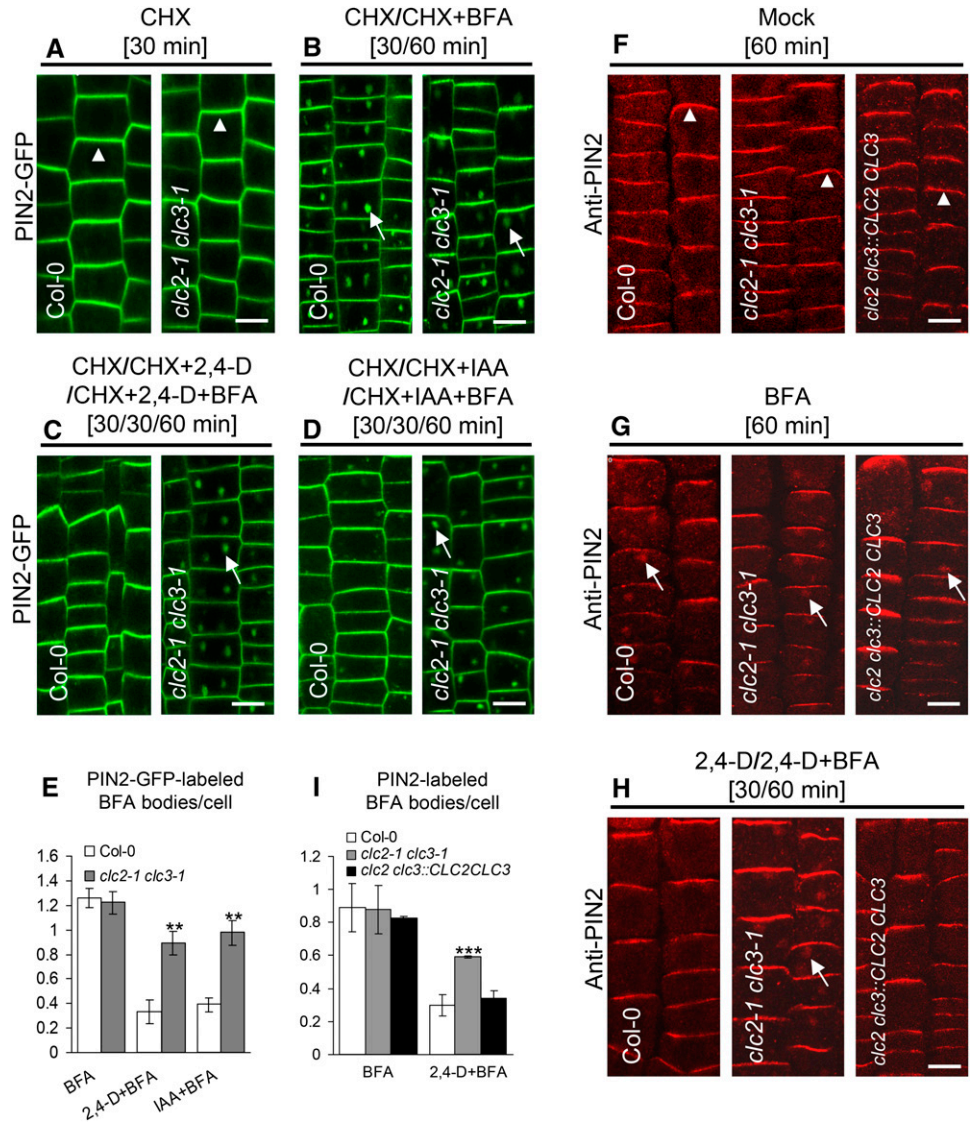

Figure 6. Impaired Auxin Inhibition of PIN2 Internalization in *clc2-1 clc3-1*.

(A) to **(D)** Auxin effect on PIN2-GFP internalization in the wild type and *clc2-1 clc3-1*.

(E) The average number of PIN2-GFP–labeled BFA bodies (**[B]** to **[D]**).

(F) to **(H)** Immunolocalization assay for auxin effect on endogenous PIN2 internalization in wild-type, *clc2-1 clc3-1*, and *clc2-1 clc3-1*::*CLC2 CLC3* rescued plants.

(I) The average number of PIN2-labeled BFA bodies (**[G]** and **[H]**).

Arrowheads indicate PM apical localization of PIN2, whereas arrows show PIN2-GFP– or PIN2-labeled in BFA bodies. Bars = 10 μm. Shown are means ± SD. Double and triple asterisks indicate $P < 0.01$ and 0.001, respectively (Student's *t* test).

Previous genetic and biochemical studies in yeast and animals have shown that CLCs contribute to the stability and trimerization of CHCs (Huang et al., 1997; Ybe et al., 2007). For example, the loss-of-function *clc1* yeast mutants show a dramatic reduction in the steady state levels of CHC (Chu et al., 1996; Huang et al., 1997), indicating that CLCs are essential for assembly and/or membrane association of CHCs. Depletion of CLCs in vitro and in vivo has also been shown to promote the spontaneous assembly and PM association of CHCs in animal cells (Liu et al., 1995, 1998). In addition, clathrin lattice assembly during the formation of CCPs is promoted via CLC-mediated CHC conformational changes (Wilbur et al., 2010) and through the interaction of CLCs with the endocytic actin binding protein, HIP-1 (Wilbur et al., 2008; Boettner et al., 2011). Thus, it is likely that CLCs possess multiple regulatory roles in the formation and disassembly of clathrin complexes in yeast and animal cells (Brodsky et al., 1991; Ybe et al., 1998, 2007). Our results suggest that plant CLCs play a similarly complex and significant role

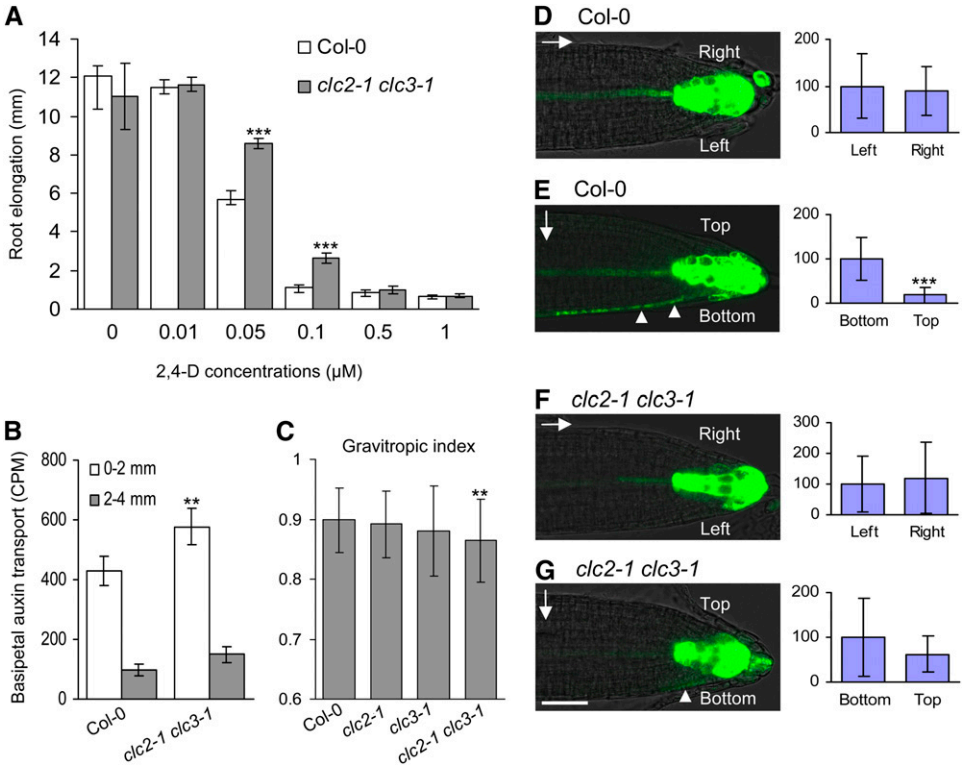

Figure 7. Alteration in Auxin Sensitivity, Auxin Transport and Distribution, and Gravity Response in *clc2-1 clc3-1*.

(A) Auxin sensitivity assay in the wild type and *clc2-1 clc3-1*.
(B) Root basipetal auxin transport assay in the wild type and *clc2-1 clc3-1*. CPM, counts per minute.
(C) Impaired root gravitropic response in *clc2-1 clc3-1*.
(D) to **(G)** The expression analysis of *DR5:GFP* for auxin distribution at the both sides of vertically grown roots (**[D]** and **[F]**) and 2-h gravistimulated roots (**[E]** and **[G]**) in the wild type and *clc2-1 clc3-1* in the left panels. The right panels show the quantitative data for the relative intensity of the GFP signals at the both sides of the roots in the left panels. Arrows and arrowheads indicate the gravity vector and the GFP signal at the bottom side of the gravistimulated roots, respectively.
Shown are means ± SD. Double asterisks indicate $P < 0.01$ (**[C]** and **[B]**); triple asterisks indicate $P < 0.001$ **(A)** and 0.0001 **(E)** (Student's *t* test; compared with the corresponding wild-type control in **[A]** to **[C]**). Bar = 50 μm.

in the regulation of assembly and/or membrane association of CHC triskelia in plants. Future studies are required to elucidate how CLCs are involved in regulating CHC membrane abundance and function in clathrin-mediated trafficking from the PM and/or TGN/EE in plants.

Although the general processes of clathrin-mediated trafficking are likely to be evolutionally conserved in all eukaryotes (Holstein, 2002; Konopka et al., 2008; Chen et al., 2011; McMahon and Boucrot, 2011), the regulation of clathrin-mediated trafficking by auxin appears to be plant specific (Robert et al., 2010). In wild-type *Arabidopsis* cells, which express three CLC isoforms, it is likely that the auxin-induced transient depletion of all CLCs causes a rapid change in the composition of clathrin triskelia, leading to transiently enhanced membrane association of CHCs (Figure 1; see Supplemental Figures 1 and 2 online) and a rapid inhibition of CME (see Supplemental Figure 12 online). In the *clc2 clc3* mutants, which constitutively lack CLC2 and CLC3, but express CLC1 (Figure 5; see Supplemental Figure 5 online), the long-term steady state levels of clathrin triskelia and/or stoichiometry of CHC and CLC subunits are likely altered, leading to impaired clathrin-mediated trafficking and auxin inhibition (Figures 4 and 6; see Supplemental Figures 10 to 13 online). The effects of transient depletion of three CLCs isoforms from the PM and TGN/EE by auxin in the wild type versus the long-term loss of CLC2 and CLC3 in the *clc2 clc3* double mutants may lead to the observed differences in PM protein internalization and CHC membrane association (Figures 1 and 4 to 6; see Supplemental Figures 2, 8, 10, and 13 online). Interestingly, we observed that auxin inhibitory effects on internalization of PM proteins in the *clc2 clc3* double mutants were significantly reduced relative to the wild type (Figure 6). Whether this is due to an alteration in the subunit composition of clathrin triskelia or misregulation of potentially a clathrin-independent internalization pathway in the *clc2 clc3* double mutant will require further experimentation, including the analysis of viable mutant lines in which all three CLC isoforms can be depleted.

Pharmacological experiments (see Supplemental Figures 2 and 6 online) revealed that the auxin-stimulated transient membrane dissociation and association of CLCs and CHCs, respectively, were not directly regulated by de novo protein synthesis and degradation processes. However, PM protein internalization remained inhibited in the presence of exogenous auxin (120 min; see Supplemental Figure 12 online), likely due to the proteasome-mediated degradation of CHCs despite the restoration of CLCs to the wild-type levels through de novo protein synthesis. These results suggest that the initial non-proteasome-dependent depletion of CLCs from membranes is likely to be the major determinant for the rapid auxin inhibition of PM protein trafficking from the PM and TGN/EE. However, further investigation is required to understand the consequences to endocytosis and TGN/EE trafficking brought on by the transient increase in membrane-associated CHC levels and its subsequent proteasome-mediated protein degradation in response to auxin.

Clathrin-Mediated Trafficking in PM Endocytosis and TGN/EE Sorting

In addition to its role in CME, clathrin is associated with the TGN/EE (Pesacreta and Lucas, 1984; Tanchak et al., 1988; Dhonukshe et al., 2007; Konopka et al., 2008; Ito et al., 2012), and the *clc2 clc3* double mutants showed decreased levels of TGN/EE-associated CHCs (see Supplemental Figures 2 and 8 online), indicating that CLCs are required for CHC recruitment to both the PM and TGN/EE.

In plant cells, the TGN/EE serves as the major protein sorting station for biosynthetic secretory proteins en route to the vacuole and PM and meanwhile receives endocytosed material from the PM that may be delivered to the vacuole for degradation or recycled back to the PM (Dettmer et al., 2006; Lam et al., 2007; Chow et al., 2008; Viotti et al., 2010). The long postulated role for CCVs that bud from the TGN/EE in vacuolar protein sorting and trafficking (Harley and Beevers, 1989) is supported by studies showing that mutants defective for the A/ENTH domain–containing protein Epsin1, which interacts with clathrin and adaptor protein 1 (AP1) (Song et al., 2006), as well as plant cells expressing a dominant-activated form of the GTPase ADP ribosylation factor 1 (ARF1), which is required for CCV protein association with membranes (Pimpl et al., 2003), have vacuolar sorting defects. However, contradictory evidence showing that overexpression of the C terminus of CHC, which inhibits CME (Dhonukshe et al., 2007), does not inhibit vacuolar protein transport (Scheuring et al., 2011) has called this model into question. Our study showing the impaired trafficking of internalized material to the vacuole lumen in the *clc2 clc3* double mutants (Figure 4; see Supplemental Figure 10 online) appears to support the role of CCVs in vacuolar trafficking, although it cannot be ruled out that the impaired vacuole delivery in the mutants is due to the initial reduction endocytosis and/or to other alterations in the balance of membrane flux between the various endocytic compartments.

An alternative, but not mutually exclusive function for TGN/EE-derived CCVs is to recycle internalized material back to the PM. Indeed, we have found that the recycling of internalized PIN2-GFP and RCI2A-GFP to the PM was inhibited in the *clc2 clc3* double mutants (Figure 4; see Supplemental Figure 10 online). Taken together, our data suggest that CLCs regulate clathrin-mediated trafficking required for PM endocytosis, recycling from the TGN/EE back to the PM, and potentially have a function in vacuolar protein trafficking.

The Role of CLCs in ABP1-Mediated Auxin Signaling

We demonstrated that the differential effects of auxin on the association of CLCs and CHCs with the PM and TGN/EE are APB1 dependent (Figure 2; see Supplemental Figure 2 online) and that CLCs play a regulatory role in ABP1-mediated auxin regulation of clathrin function in PM protein internalization (Figures 5 and 6; see Supplemental Figures 13 online). However, the molecular mechanism by which auxin signaling is transduced between extracellular- and/or endoplasmic reticulum–localized APB1 and PM- and TGN/EE-localized CLCs remains to be elucidated.

One candidate involved in this signaling pathway may be the Rho-like GTPase ROP6, which has been demonstrated to participate in ABP1-mediated auxin inhibition of PIN1 and PIN2 endocytosis in *Arabidopsis* roots (Chen et al., 2012; Lin et al., 2012). Similar to the *clc2-1 clc3-1* double mutants (Figures 6 and 7), *rop6-1* and *rop6-2* mutants display a diminished root gravity response and a reduction in auxin-mediated inhibition of PIN internalization (Chen et al., 2012; Lin et al., 2012), suggesting that CLCs might be downstream targets of ROP6-mediated signaling. Further studies showing a physical and/or genetic link between ROP6 and CLCs are required to support this model.

The Role of CLCs in Plant Development

Our phenotypic analyses of the *clc2-1* and *clc3-1* single mutants and *clc2 clc3* double mutants (Figures 3, 4, and 7) indicated that CLC2 and CLC3 are functionally redundant and necessary for auxin regulation of plant development. Likewise, the levels of PM- and TGN/EE-associated CLC1 were found to be modulated by exogenous auxin. However, due to the gametophytic lethality of the *clc1-1* mutation, it remains to be determined whether CLC1 is functionally redundant with CLC2 and CLC3.

Our data therefore suggest that the rapid depletion of CLCs is essential for the fine-tuning and rapid inhibition of CME by auxin and for the regulation of auxin efflux via properly localized PINs. As a consequence, some of the phenotypes observed in the *clc2 clc3* double mutants are likely to be directly related to defects in auxin transport and distribution (Figures 3, 4, and 7). However, we expect that the *clc2 clc3* double mutants will have additional phenotypes as the CLCs appear to be required for both general CME of PM proteins and the trafficking of proteins from the TGN/EE. Our results reveal that CLCs play a crucial, regulatory role in plant developmental processes. Further analysis of the *clc2 clc3* double mutants and the roles of CLCs in CME and other clathrin-mediated trafficking events will provide a greater understanding of the functional roles of clathrin in plant development, nutrient uptake, and responses to environmental cues.

METHODS

Plant Materials and Growth Conditions

The following transgenic lines and mutants were used in this study: *ProCLC2*:*CLC2-GFP* (Konopka et al., 2008; Ito et al., 2012), *DR5*:*GFP* (Benková et al., 2003), *DR5*:*GUS* (Benková et al., 2003), *ProPIN1*:*PIN1-GFP* (Heisler et al., 2005), *ProPIN2*:*PIN2-GFP* (Xu and Scheres, 2005), *ProPIN3*:*PIN3-GFP* (Blilou et al., 2005), *ProPIN7*:*PIN7-GFP* (Blilou et al., 2005), and *ProRCI2A*:*RCI2A-GFP* (Cutler et al., 2000) transgenic lines as well as *tir1-1 afb1-1 afb2-1 afb3-1* (*tir1 afb1*, *2*, *3*) (Dharmasiri et al., 2005), *axr1-12* (Leyser et al., 1993), and *axr6-3* mutants (Quint et al., 2005). Mutant lines from the Arabidopsis Biological Resource Center (ABRC) are as follows: *abp1-5* (CS91358), *clc1-1* (SALK_147101), *clc2-1* (SALK_016049), *clc3-1* (CS100219), *chc1-1* (SALK_112213), *chc1-2* (SALK_103252), *chc2-1* (SALK_028826), *chc2-2* (SALK_042321), *chc2-3* (CS850328), and *pin2* (SALK_144447). Homozygous mutant lines were isolated and identified by PCR and RT-PCR or sequencing-based assays (see Supplemental Table 2 online). The *clc2-1 clc3-1* double mutants were generated by crossing with each other and a PCR-based assay.

Seeds were surface sterilized and imbibed for 3 d at 4°C in dark and then sown onto 0.5× Murashige and Skoog (MS) 1.5% (w/v) agar plates. Seedlings were vertically grown on plates in a climate-controlled growth room (22/20°C day/night temperature, 16/8-h photoperiod, and 80 μE s^{-1} m^{-2} light intensity). Five-day-old seedlings with healthy roots were used in this study.

Chemical Solutions and Treatments

All reagents unless specified were from Sigma-Aldrich. All chemical stock solutions were prepared as follows: DMSO was used to dissolve CHX (50 mM), MG132 (50 mM), 5-F-IAA (20 mM), BFA (50 mM; Invitrogen), tyrphostin A23 (30 mM), and tyrphostin A51 (30 mM). IAA (10 mM), 2,4-D (10 mM), 1-NAA (10 mM), and 2-NAA (10 mM) were first dissolved in a few drops of 1 M KOH and then diluted with water. Unless otherwise indicated, final working concentrations were 50 μM for CHX, MG132, and BFA, 30 μM for tyrphostin A23 and A51, 20 μM for IAA, 2-NAA, and 5-F-IAA, and 10 μM for 2,4-D and 1-NAA. All pretreatments with various chemicals were for 30 min, and treatment time is indicated in the text. All experiments were performed in MS basal salts with minimal organics (Sigma-Aldrich) supplemented with 1% (w/v) Suc and 0.05% (w/v) MES-KOH, pH 5.6 (0.5× MS), liquid medium, except where specified. The pH of the medium after addition of chemical stock solutions was confirmed to be ~5.6 to 5.62.

Constructs and Complementation Test

The constructs of *35S*:*CLC1-GFP*, *ProCLC2*:*CLC2*, and *ProCLC3*:*CLC3* were generated using PCR, restriction digestion, and ligation with transformation vectors. The construct of *35S*::*GFP-ABP1*$^{\Delta KDEL}$ was generated as previously described by Robert et al. (2010) and transformed into Columbia-0.

To test the complementation for the *clc2-1 clc3-1* double mutants, *ProCLC2*:*CLC2* and *ProCLC3*:*CLC3* were transformed into the *clc2-1 clc3-1* double homozygous lines, respectively. After recovering T1 plants (*clc2-1 clc3-1*::*CLC2* and *clc2-1 clc3-1*::*CLC3*), they were crossed with each other to generate the *clc2-1 clc3-1*::*CLC2 CLC3* plants by PCR- and RT-PCR–based assays. All primer sequences are indicated in Supplemental Table 2 online.

Polyclonal Antibodies

Polyclonal antibodies (anti-AtCLC1, anti-AtCLC2, anti-AtCLC3, anti-AtCHC [which cross-reacts with both CHC1 and CHC2 isoforms], and anti-AtPIN2) were raised in rabbits using synthesized peptides related to each protein (see Supplemental Table 3 online) coupled with keyhole limpet hemocyanin containing an additional N-terminal Cys (Huabio). Antibodies were affinity purified using immobilized peptide affinity columns, and their specificity was verified as shown in Supplemental Figures 9C and 14 online.

Cytology and Immunodetection

Immunolocalization studies were preformed in primary roots as described Sauer et al. (2006b). Primary antibodies, against CLC1, CLC2, CLC3, CHC, and PIN2, were detected using Cy3-labeled anti-rabbit secondary antibodies (Sigma-Aldrich).

Images were captured using CLSM (Leica TCS SP5 AOBS). Excitation wavelengths were 488 nm (argon laser) for GFP and 561 nm (diode laser) for Cy3. Emission was detected at 496 to 532 nm for GFP and 550 to 570 nm for Cy3. For quantitative measurement of fluorescence intensities, laser, pinhole, and gain settings of the confocal microscope were identical among different treatments or genotypes.

To measure the intensities of fluorescence signals at the PM and TGN/EE, digital images were analyzed using Image J (http://rsb.info.nih.gov/ij), and the relative fluorescence intensities were presented as percentages of mock controls as previously described (Sauer et al., 2006a; Robert et al., 2010). As the intracellular pools of CLCs and CHCs are predominantly associated with the TGN/EE (Dhonukshe et al., 2007; Konopka et al., 2008; Robert et al., 2010), the levels of TGN/EE-associated CLCs and CHCs were determined by measuring total intracellular fluorescence intensities of GFP-fused or Cy3-labeled secondary antibody detected proteins. For measurements of BFA-induced internalization of PM-localized proteins, the levels of internalized GFP-fused or Cy3-labeled secondary antibody detected PM proteins were presented as the average number of fluorescence-labeled BFA bodies per cell (Robert et al., 2010). Due to internalized GFP-fused PM proteins predominantly accumulating in the vacuolar lumen 2 to 4 h after dark treatments (Kleine-Vehn et al., 2008; Laxmi et al., 2008), average intensities of vacuolar GFP-fused PM proteins were calculated by measuring the total intracellular signal using Image J, and the relative intensities were presented as percentages of wild-type controls. In all above quantification of the CLSM data, the minimum numbers of 15 individual roots and 10 to 15 cells per root from three independent experiments were analyzed for each time point treatment. A Student's *t* test (paired with two-tailed distribution) was used in statistical analysis for all the quantitative data.

Root Hair Polarity and LRP

For the root hair polarity analysis, relative positions of hair initiation were indicated as apical-basal initiation ratio = initiation length (μm)/cell length (μm) (Grebe et al., 2002). Initiation length indicated the distance from the central of the root hair base to the basal cell wall of the cell. The numbers 0 and 1 represent the basal and apical sides of the trichoblast cell, respectively. The apical-basal initiation ratios of 10 trichoblast cells per root were calculated. The apical-basal initiation ratios of ~300 trichoblast cells from 30 roots per genotype from three independent experiments were used to analyze for class distributions. Fisher's exact test applying the "Fisher 2 by 5" program (http://www.quantitativeskills.com/sisa/) was used to analyze independence of distributions.

For the LRP assay, *DR5*:*GUS* was used to examine LRP formation (Benková et al., 2003). Seven- to 10-day-old seedlings were incubated in the X-gluc staining solution (10 mM EDTA, 0.1% Triton X-100, 2 mM Fe^{2+}CN, 2 mM Fe^{3+}CN, 100 μg/mL chloramphenicol, and 1 mg/mL X-gluc in 50 mM phosphate buffer, pH 7.0) at 37°C overnight. After staining, tissues were cleared using 70% ethanol to remove chlorophyll for tissue localization and photographed using a dissecting microscope. The LRP density (the ratio of the LRP number to the root length) of 30 seedling roots from three independent experiments was used to evaluate LRP formation pattern for each age per genotype.

Auxin Sensitivity, Transport and Distribution, and Root Gravitropism

For the auxin sensitivity assay, 5-d-old vertically grown seedlings were transferred from 0.5× MS agar plates to 0.5× MS agar plates with different 2,4-D concentrations (0, 0.01, 0.05, 0.1, 0.5, and 1 μM). Root elongation measurements were performed after 3 d. To determine the distribution of auxin in roots, the *DR5*:*GFP* auxin-responsive reporter (Benková et al., 2003) was introgressed into the *clc2-1 clc3-1* double mutant lines, and *DR5*:*GFP* expression within root tips was analyzed 2 h after gravistimulation by CLSM. Root gravitropic response was evaluated using the gravitropic index, which was defined as the ratio between the vertical distance/ordinate from the root tip to the root base and the root length (Grabov et al., 2005). For the quantification of above experimental data, digital images collected from 30 seedlings per genotype from three independent experiments were analyzed using Image J. For the quantification of root and hypocotyl lengths, digital images of 45 seedlings per genotype from three independent experiments were collected and were analyzed using Image J. A Student's *t* test (paired with two-tailed distribution) was used in statistical analysis for all the quantitative data.

For the root basipetal auxin transport assay, 10 5-d-old light-grown seedlings were transferred to plates containing 0.5× MS 1.5% (w/v) agar media and incubated for 1 h. Agar blocks (1.25%) of 1 mm in diameter containing the same growth medium supplemented with 100 nM tritium-labeled IAA (^{3}H-IAA) were placed next to root tips. After incubation for 1.5 h in dark, agar blocks were removed. Root tips of ~0.3 mm in length were excised and discarded. Two consecutive 2-mm root segments were then excised from the remaining root and placed separately into two scintillation vials. Each vial contained 2 mL of scintillation fluid. The amounts of radioactivity in the two root segments were pooled from 10 roots and measured using a Perkin-Elmer 1450 Microbeta scintillation counter for 1 min. The experiments were repeated three times, and the data were statistically evaluated using a Student's *t* test (paired with two-tailed distribution).

Accession Numbers

Sequence data from this article can be found in the Arabidopsis Genome Initiative under the following accession numbers: *CLC1* (At2g20760), *CLC2* (At2g40060), *CLC3* (At3g51890), *CHC1* (At3g11130), *CHC2* (At3g08530), *PIN2* (AT5g57090), and *ABP1* (AT4g02980).

Supplemental Data

The following materials are available in the online version of this article.

Supplemental Figure 1. CLSM Imaging of Membrane-Associated CLC-GFP in the Presence of Exogenous Auxin.

Supplemental Figure 2. Immunoblot Analysis of Membrane-Associated CLC and CHC Levels.

Supplemental Figure 3. Analysis of the Differential Auxin Regulation of CHCs and CLC1-GFP in Individual Cells.

Supplemental Figure 4. Effects of IAA, 1-NAA, and Their Analogs on Membrane-Associated CLC and CHC Levels.

Supplemental Figure 5. qRT-PCR Analysis of Transcriptional Levels of *CHCs* and *CLCs*.

Supplemental Figure 6. Effects of Cycloheximide and MG132 on Membrane-Associated CLC1-GFP and CHC Levels.

Supplemental Figure 7. Differential Auxin Regulation of CLC1 and CHC Membrane Association Is $SCF^{TIR1/AFB}$ Independent.

Supplemental Figure 8. Immunolocalization Analysis of Membrane-Associated CLC1 and CHC Levels in the Wild Type and Auxin-Signaling Mutants.

Supplemental Figure 9. Molecular and Phenotypic Characterization of *clc2-1*, *clc3-1*, and Their Double Mutants and Rescued Lines.

Supplemental Figure 10. CME and Intracellular Trafficking of RCI2A-GFP.

Supplemental Figure 11. FM4-64 Internalization and Auxin Effect on PIN2-GFP PM Abundance.

Supplemental Figure 12. Auxin Inhibition of PM-Protein Internalization.

Supplemental Figure 13. Reduced Auxin Inhibitory Effect on Internalization of PM Proteins in *clc2-1 clc3-1*.

Supplemental Figure 14. Analysis of the Specificity of Antibodies Used for Immunolocalization Studies.

Supplemental Table 1. PCR Primer Sequences for Real-Time Quantitative RT-PCR.

Supplemental Table 2. PCR Primer Sequences for Genotyping, RT-PCR, and Cloning.

Supplemental Table 3. Information for Antibodies.

ACKNOWLEDGMENTS

We thank the two anonymous reviewers for their critical and constructive comments that led to significant improvement of this work, the ABRC at Ohio State University for seed stocks, and Chunyuan Huang, Kendal D. Hirschi, and Zhukuan Cheng for critical reading of the article. This work was supported by the National Natural Science Foundation of China (No. 30970255 and No. 31171520), by the Zhejiang Provincial Excellent Youth Foundation of China (No. R3100175), and by the Zhejiang Provincial Qianjiang Talents Program of China (No. 2010R10085). S.Y.B. was supported by a Vilas Associate Award (University of Wisconsin, Madison, Graduate School) and the National Science Foundation (No. 1121998).

AUTHOR CONTRIBUTIONS

C.W., B.M., J.L., C.L., S.Y.B., and J.P. conceived the study and designed the experiments. C.W., X.Y., Q.C., N.J., W.F., and J.P. carried out the experiments. C.W., C.L., S.Y.B., and J.P. analyzed the data. C.W., J.L., C.L., S.Y.B., and J.P. wrote the article.

Received December 10, 2012; revised January 21, 2013; accepted January 31, 2013; published February 19, 2013.

REFERENCES

Abas, L., Benjamins, R., Malenica, N., Paciorek, T., Wiśniewska, J., Moulinier-Anzola, J.C., Sieberer, T., Friml, J., and Luschnig, C. (2006). Intracellular trafficking and proteolysis of the *Arabidopsis* auxin-efflux facilitator PIN2 are involved in root gravitropism. Nat. Cell Biol. **8:** 249–256. Erratum. Nat. Cell Biol. **8:** 424.

Backues, S.K., Korasick, D.A., Heese, A., and Bednarek, S.Y. (2010). The *Arabidopsis* dynamin-related protein2 family is essential for gametophyte development. Plant Cell **22:** 3218–3231.

Banbury, D.N., Oakley, J.D., Sessions, R.B., and Banting, G. (2003). Tyrphostin A23 inhibits internalization of the transferrin receptor by perturbing the interaction between tyrosine motifs and the medium chain subunit of the AP-2 adaptor complex. J. Biol. Chem. **278:** 12022–12028.

Barberon, M., Zelazny, E., Robert, S., Conéjéro, G., Curie, C., Friml, J., and Vert, G. (2011). Monoubiquitin-dependent endocytosis of the iron-regulated transporter 1 (IRT1) transporter controls iron uptake in plants. Proc. Natl. Acad. Sci. USA **108:** E450–E458.

Baster, P., Robert, S., Kleine-Vehn, J., Vanneste, S., Kania, U., Grunewald, W., De Rybel, B., Beeckman, T., and Friml, J. (2012). SCF($^{TIR1/AFB}$)-auxin signalling regulates PIN vacuolar trafficking and auxin fluxes during root gravitropism. EMBO J. **32:** 260–274.

Benková, E., Michniewicz, M., Sauer, M., Teichmann, T., Seifertová, D., Jürgens, G., and Friml, J. (2003). Local, efflux-dependent auxin gradients as a common module for plant organ formation. Cell **115:** 591–602.

Blakeslee, J.J., et al. (2007). Interactions among PIN-FORMED and P-glycoprotein auxin transporters in *Arabidopsis*. Plant Cell **19:** 131–147.

Blilou, I., Xu, J., Wildwater, M., Willemsen, V., Paponov, I., Friml, J., Heidstra, R., Aida, M., Palme, K., and Scheres, B. (2005). The PIN auxin efflux facilitator network controls growth and patterning in *Arabidopsis* roots. Nature **433:** 39–44.

Boettner, D.R., Friesen, H., Andrews, B., and Lemmon, S.K. (2011). Clathrin light chain directs endocytosis by influencing the binding of the yeast Hip1R homologue, Sla2, to F-actin. Mol. Biol. Cell **22:** 3699–3714.

Brodsky, F.M., Hill, B.L., Acton, S.L., Näthke, I., Wong, D.H., Ponnambalam, S., and Parham, P. (1991). Clathrin light chains: Arrays of protein motifs that regulate coated-vesicle dynamics. Trends Biochem. Sci. **16:** 208–213.

Chen, X., Irani, N.G., and Friml, J. (2011). Clathrin-mediated endocytosis: The gateway into plant cells. Curr. Opin. Plant Biol. **14:** 674–682.

Chen, X., Naramoto, S., Robert, S., Tejos, R., Löfke, C., Lin, D., Yang, Z., and Friml, J. (2012). ABP1 and ROP6 GTPase signaling regulate clathrin-mediated endocytosis in *Arabidopsis* roots. Curr. Biol. **22:** 1326–1332.

Chow, C.M., Neto, H., Foucart, C., and Moore, I. (2008). Rab-A2 and Rab-A3 GTPases define a trans-golgi endosomal membrane domain in *Arabidopsis* that contributes substantially to the cell plate. Plant Cell **20:** 101–123.

Chu, D.S., Pishvaee, B., and Payne, G.S. (1996). The light chain subunit is required for clathrin function in *Saccharomyces cerevisiae*. J. Biol. Chem. **271:** 33123–33130.

Cutler, S.R., Ehrhardt, D.W., Griffitts, J.S., and Somerville, C.R. (2000). Random GFP:cDNA fusions enable visualization of subcellular structures in cells of *Arabidopsis* at a high frequency. Proc. Natl. Acad. Sci. USA **97:** 3718–3723.

Dettmer, J., Hong-Hermesdorf, A., Stierhof, Y.D., and Schumacher, K. (2006). Vacuolar H+-ATPase activity is required for endocytic and secretory trafficking in *Arabidopsis*. Plant Cell **18:** 715–730.

Dharmasiri, N., Dharmasiri, S., and Estelle, M. (2005). The F-box protein TIR1 is an auxin receptor. Nature **435:** 441–445.

Dhonukshe, P., Aniento, F., Hwang, I., Robinson, D.G., Mravec, J., Stierhof, Y.D., and Friml, J. (2007). Clathrin-mediated constitutive endocytosis of PIN auxin efflux carriers in *Arabidopsis*. Curr. Biol. **17:** 520–527.

Dhonukshe, P., et al. (2008). Generation of cell polarity in plants links endocytosis, auxin distribution and cell fate decisions. Nature **456:** 962–966.

Ding, Z., Galván-Ampudia, C.S., Demarsy, E., Łangowski, Ł., Kleine-Vehn, J., Fan, Y., Morita, M.T., Tasaka, M., Fankhauser, C., Offringa, R., and Friml, J. (2011). Light-mediated polarization of the PIN3 auxin transporter for the phototropic response in *Arabidopsis*. Nat. Cell Biol. **13:** 447–452.

Effendi, Y., Rietz, S., Fischer, U., and Scherer, G.F.E. (2011). The heterozygous abp1/ABP1 insertional mutant has defects in functions requiring polar auxin transport and in regulation of early auxin-regulated genes. Plant J. **65:** 282–294.

Friml, J., Vieten, A., Sauer, M., Weijers, D., Schwarz, H., Hamann, T., Offringa, R., and Jürgens, G. (2003). Efflux-dependent auxin gradients establish the apical-basal axis of *Arabidopsis*. Nature **426:** 147–153.

Gälweiler, L., Guan, C., Müller, A., Wisman, E., Mendgen, K., Yephremov, A., and Palme, K. (1998). Regulation of polar auxin transport by AtPIN1 in *Arabidopsis* vascular tissue. Science **282:** 2226–2230.

Geisler, M., and Murphy, A.S. (2006). The ABC of auxin transport: The role of p-glycoproteins in plant development. FEBS Lett. **580:** 1094–1102.

Geldner, N., Anders, N., Wolters, H., Keicher, J., Kornberger, W., Muller, P., Delbarre, A., Ueda, T., Nakano, A., and Jürgens, G. (2003). The *Arabidopsis* GNOM ARF-GEF mediates endosomal recycling, auxin transport, and auxin-dependent plant growth. Cell **112:** 219–230.

Geldner, N., Friml, J., Stierhof, Y.D., Jürgens, G., and Palme, K. (2001). Auxin transport inhibitors block PIN1 cycling and vesicle trafficking. Nature **413:** 425–428.

Geldner, N., Hyman, D.L., Wang, X., Schumacher, K., and Chory, J. (2007). Endosomal signaling of plant steroid receptor kinase BRI1. Genes Dev. **21:** 1598–1602.

Grabov, A., Ashley, M.K., Rigas, S., Hatzopoulos, P., Dolan, L., and Vicente-Agullo, F. (2005). Morphometric analysis of root shape. New Phytol. **165:** 641–651.

Grebe, M., Friml, J., Swarup, R., Ljung, K., Sandberg, G., Terlou, M., Palme, K., Bennett, M.J., and Scheres, B. (2002). Cell polarity signaling in *Arabidopsis* involves a BFA-sensitive auxin influx pathway. Curr. Biol. **12:** 329–334.

Harley, S.M., and Beevers, L. (1989). Coated vesicles are involved in the transport of storage proteins during seed development in *Pisum sativum* L. Plant Physiol. **91:** 674–678.

Heisler, M.G., Ohno, C., Das, P., Sieber, P., Reddy, G.V., Long, J.A., and Meyerowitz, E.M. (2005). Patterns of auxin transport and gene expression during primordium development revealed by live imaging of the *Arabidopsis* inflorescence meristem. Curr. Biol. **15:** 1899–1911.

Holstein, S.E.H. (2002). Clathrin and plant endocytosis. Traffic **3:** 614–620.

Huang, K.M., Gullberg, L., Nelson, K.K., Stefan, C.J., Blumer, K., and Lemmon, S.K. (1997). Novel functions of clathrin light chains: Clathrin heavy chain trimerization is defective in light chain-deficient yeast. J. Cell Sci. **110:** 899–910.

Irani, N.G., et al. (2012). Fluorescent castasterone reveals BRI1 signaling from the plasma membrane. Nat. Chem. Biol. **8:** 583–589.

Ito, E., Fujimoto, M., Ebine, K., Uemura, T., Ueda, T., and Nakano, A. (2012). Dynamic behavior of clathrin in *Arabidopsis thaliana* unveiled by live imaging. Plant J. **69:** 204–216.

Kang, B.H., Rancour, D.M., and Bednarek, S.Y. (2003). The dynamin-like protein ADL1C is essential for plasma membrane maintenance during pollen maturation. Plant J. **35:** 1–15.

Kitakura, S., Vanneste, S., Robert, S., Löfke, C., Teichmann, T., Tanaka, H., and Friml, J. (2011). Clathrin mediates endocytosis and polar distribution of PIN auxin transporters in *Arabidopsis*. Plant Cell **23:** 1920–1931.

Kleine-Vehn, J., Leitner, J., Zwiewka, M., Sauer, M., Abas, L., Luschnig, C., and Friml, J. (2008). Differential degradation of PIN2 auxin efflux carrier by retromer-dependent vacuolar targeting. Proc. Natl. Acad. Sci. USA **105:** 17812–17817.

Konopka, C.A., Backues, S.K., and Bednarek, S.Y. (2008). Dynamics of *Arabidopsis* dynamin-related protein 1C and a clathrin light chain at the plasma membrane. Plant Cell **20:** 1363–1380.

Lam, S.K., Cai, Y., Tse, Y.C., Wang, J., Law, A.H., Pimpl, P., Chan, H.Y., Xia, J., and Jiang, L. (2009). BFA-induced compartments from the Golgi apparatus and trans-Golgi network/early endosome are distinct in plant cells. Plant J. **60:** 865–881.

Lam, S.K., Tse, Y.C., Robinson, D.G., and Jiang, L. (2007). Tracking down the elusive early endosome. Trends Plant Sci. **12:** 497–505.

Laxmi, A., Pan, J., Morsy, M., and Chen, R. (2008). Light plays an essential role in intracellular distribution of auxin efflux carrier PIN2 in *Arabidopsis thaliana*. PLoS ONE **3:** e1510.

Leborgne-Castel, N., Lherminier, J., Der, C., Fromentin, J., Houot, V., and Simon-Plas, F. (2008). The plant defense elicitor cryptogein stimulates clathrin-mediated endocytosis correlated with reactive oxygen species production in bright yellow-2 tobacco cells. Plant Physiol. **146:** 1255–1266.

Leyser, H.M.O., Lincoln, C.A., Timpte, C., Lammer, D., Turner, J., and Estelle, M. (1993). *Arabidopsis* auxin-resistance gene AXR1 encodes a protein related to ubiquitin-activating enzyme E1. Nature **364:** 161–164.

Leyser, O. (2011). Auxin, self-organisation, and the colonial nature of plants. Curr. Biol. **21:** R331–R337.

Lin, D., et al. (2012). A ROP GTPase-dependent auxin signaling pathway regulates the subcellular distribution of PIN2 in *Arabidopsis* roots. Curr. Biol. **22:** 1319–1325.

Liu, S.H., Marks, M.S., and Brodsky, F.M. (1998). A dominant-negative clathrin mutant differentially affects trafficking of molecules with distinct sorting motifs in the class II major histocompatibility complex (MHC) pathway. J. Cell Biol. **140:** 1023–1037.

Liu, S.H., Wong, M.L., Craik, C.S., and Brodsky, F.M. (1995). Regulation of clathrin assembly and trimerization defined using recombinant triskelion hubs. Cell **83:** 257–267.

Liu, Z.B., Ulmasov, T., Shi, X., Hagen, G., and Guilfoyle, T.J. (1994). Soybean GH3 promoter contains multiple auxin-inducible elements. Plant Cell **6:** 645–657.

McMahon, H.T., and Boucrot, E. (2011). Molecular mechanism and physiological functions of clathrin-mediated endocytosis. Nat. Rev. Mol. Cell Biol. **12:** 517–533.

Medina, J., Ballesteros, M.L., and Salinas, J. (2007). Phylogenetic and functional analysis of *Arabidopsis RCI2* genes. J. Exp. Bot. **58:** 4333–4346.

Mettlen, M., Stoeber, M., Loerke, D., Antonescu, C.N., Danuser, G., and Schmid, S.L. (2009). Endocytic accessory proteins are functionally distinguished by their differential effects on the maturation of clathrin-coated pits. Mol. Biol. Cell **20:** 3251–3260.

Mravec, J., et al. (2011). Cell plate restricted association of DRP1A and PIN proteins is required for cell polarity establishment in *Arabidopsis*. Curr. Biol. **21:** 1055–1060.

Newpher, T.M., Idrissi, F.Z., Geli, M.I., and Lemmon, S.K. (2006). Novel function of clathrin light chain in promoting endocytic vesicle formation. Mol. Biol. Cell **17:** 4343–4352.

Paciorek, T., Zazímalová, E., Ruthardt, N., Petrásek, J., Stierhof, Y.D., Kleine-Vehn, J., Morris, D.A., Emans, N., Jürgens, G., Geldner, N., and Friml, J. (2005). Auxin inhibits endocytosis and promotes its own efflux from cells. Nature **435:** 1251–1256.

Pan, J., Fujioka, S., Peng, J., Chen, J., Li, G., and Chen, R. (2009). The E3 ubiquitin ligase $^{SCFTIR1/AFB}$ and membrane sterols play key roles in auxin regulation of endocytosis, recycling, and plasma membrane accumulation of the auxin efflux transporter PIN2 in *Arabidopsis thaliana*. Plant Cell **21:** 568–580.

Pesacreta, T.C., and Lucas, W.J. (1984). Plasma membrane coat and a coated vesicle-associated reticulum of membranes: Their structure and possible interrelationship in *Chara corallina*. J. Cell Biol. **98:** 1537–1545.

Petrásek, J., et al. (2006). PIN proteins perform a rate-limiting function in cellular auxin efflux. Science **312:** 914–918.

Pimpl, P., Hanton, S.L., Taylor, J.P., Pinto-daSilva, L.L., and Denecke, J. (2003). The GTPase ARF1p controls the sequence-specific vacuolar sorting route to the lytic vacuole. Plant Cell **15:** 1242–1256.

Quint, M., Ito, H., Zhang, W., and Gray, W.M. (2005). Characterization of a novel temperature-sensitive allele of the CUL1/AXR6 subunit of SCF ubiquitin-ligases. Plant J. **43:** 371–383.

Rashotte, A.M., Brady, S.R., Reed, R.C., Ante, S.J., and Muday, G.K. (2000). Basipetal auxin transport is required for gravitropism in roots of *Arabidopsis*. Plant Physiol. **122:** 481–490.

Robert, S., et al. (2010). ABP1 mediates auxin inhibition of clathrin-dependent endocytosis in *Arabidopsis*. Cell **143:** 111–121.

Royle, S.J. (2006). The cellular functions of clathrin. Cell. Mol. Life Sci. **63:** 1823–1832.

Sauer, M., Balla, J., Luschnig, C., Wisniewska, J., Reinöhl, V., Friml, J., and Benková, E. (2006a). Canalization of auxin flow by Aux/IAA-ARF-dependent feedback regulation of PIN polarity. Genes Dev. **20:** 2902–2911.

Sauer, M., and Kleine-Vehn, J. (2011). AUXIN BINDING PROTEIN1: The outsider. Plant Cell **23:** 2033–2043.

Sauer, M., Paciorek, T., Benková, E., and Friml, J. (2006b). Immunocytochemical techniques for whole-mount in situ protein localization in plants. Nat. Protoc. **1:** 98–103.

Scheuring, D., Viotti, C., Krüger, F., Künzl, F., Sturm, S., Bubeck, J., Hillmer, S., Frigerio, L., Robinson, D.G., Pimpl, P., and Schumacher, K. (2011). Multivesicular bodies mature from the trans-Golgi network/early endosome in *Arabidopsis*. Plant Cell **23:** 3463–3481.

Shin, H., Shin, H.S., Guo, Z., Blancaflor, E.B., Masson, P.H., and Chen, R. (2005). Complex regulation of *Arabidopsis* AGR1/PIN2-mediated root gravitropic response and basipetal auxin transport by cantharidin-sensitive protein phosphatases. Plant J. **42:** 188–200.

Sieberer, T., Seifert, G.J., Hauser, M.T., Grisafi, P., Fink, G.R., and Luschnig, C. (2000). Post-transcriptional control of the *Arabidopsis* auxin efflux carrier EIR1 requires AXR1. Curr. Biol. **10:** 1595–1598.

Song, J., Lee, M.H., Lee, G.J., Yoo, C.M., and Hwang, I. (2006). *Arabidopsis* EPSIN1 plays an important role in vacuolar trafficking of soluble cargo proteins in plant cells via interactions with clathrin, AP-1, VTI11, and VSR1. Plant Cell **18:** 2258–2274.

Sun, J., Chen, Q., Qi, L., Jiang, H., Li, S., Xu, Y., Liu, F., Zhou, W., Pan, J., Li, X., Palme, K., and Li, C. (2011). Jasmonate modulates endocytosis and plasma membrane accumulation of the *Arabidopsis* PIN2 protein. New Phytol. **191:** 360–375.

Swarup, R., Kramer, E.M., Perry, P., Knox, K., Leyser, H.M.O., Haseloff, J., Beemster, G.T.S., Bhalerao, R., and Bennett, M.J. (2005). Root gravitropism requires lateral root cap and epidermal cells for transport and response to a mobile auxin signal. Nat. Cell Biol. **7:** 1057–1065.

Tanchak, M.A., Rennie, P.J., and Fowke, L.C. (1988). Ultrastrucure of the partially coated reticulum and dictyosomes during endocytosis by soybean protoplasts. Planta **175:** 433–441.

Titapiwatanakun, B., et al. (2009). ABCB19/PGP19 stabilises PIN1 in membrane microdomains in *Arabidopsis*. Plant J. **57:** 27–44.

Van Damme, D., Gadeyne, A., Vanstraelen, M., Inzé, D., Van Montagu, M.C.E., De Jaeger, G., Russinova, E., and Geelen, D. (2011). Adaptin-like protein TPLATE and clathrin recruitment during plant somatic cytokinesis occurs via two distinct pathways. Proc. Natl. Acad. Sci. USA **108:** 615–620.

Vieten, A., Vanneste, S., Wiśniewska, J., Benková, E., Benjamins, R., Beeckman, T., Luschnig, C., and Friml, J. (2005). Functional

redundancy of PIN proteins is accompanied by auxin-dependent cross-regulation of PIN expression. Development **132:** 4521–4531.

Viotti, C., et al. (2010). Endocytic and secretory traffic in *Arabidopsis* merge in the trans-Golgi network/early endosome, an independent and highly dynamic organelle. Plant Cell **22:** 1344–1357.

Wan, Y., Jasik, J., Wang, L., Hao, H., Volkmann, D., Menzel, D., Mancuso, S., Baluška, F., and Lin, J. (2012). The signal transducer NPH3 integrates the phototropin1 photosensor with PIN2-based polar auxin transport in *Arabidopsis* root phototropism. Plant Cell **24:** 551–565.

Wilbur, J.D., Chen, C.Y., Manalo, V., Hwang, P.K., Fletterick, R.J., and Brodsky, F.M. (2008). Actin binding by Hip1 (huntingtin-interacting protein 1) and Hip1R (Hip1-related protein) is regulated by clathrin light chain. J. Biol. Chem. **283:** 32870–32879.

Wilbur, J.D., Hwang, P.K., Ybe, J.A., Lane, M., Sellers, B.D., Jacobson, M.P., Fletterick, R.J., and Brodsky, F.M. (2010). Conformation switching of clathrin light chain regulates clathrin lattice assembly. Dev. Cell **18:** 841–848.

Wisniewska, J., Xu, J., Seifertová, D., Brewer, P.B., Ruzicka, K., Blilou, I., Rouquié, D., Benková, E., Scheres, B., and Friml, J. (2006). Polar PIN localization directs auxin flow in plants. Science **312:** 883.

Xu, J., and Scheres, B. (2005). Dissection of *Arabidopsis* ADP-RIBOSYLATION FACTOR 1 function in epidermal cell polarity. Plant Cell **17:** 525–536.

Xu, T., Wen, M., Nagawa, S., Fu, Y., Chen, J.G., Wu, M.J., Perrot-Rechenmann, C., Friml, J., Jones, A.M., and Yang, Z. (2010). Cell surface- and rho GTPase-based auxin signaling controls cellular interdigitation in *Arabidopsis*. Cell **143:** 99–110.

Ybe, J.A., Greene, B., Liu, S.H., Pley, U., Parham, P., and Brodsky, F.M. (1998). Clathrin self-assembly is regulated by three light-chain residues controlling the formation of critical salt bridges. EMBO J. **17:** 1297–1303.

Ybe, J.A., Perez-Miller, S., Niu, Q., Coates, D.A., Drazer, M.W., and Clegg, M.E. (2007). Light chain C-terminal region reinforces the stability of clathrin heavy chain trimers. Traffic **8:** 1101–1110.

Zhao, Y., Yan, A., Feijó, J.A., Furutani, M., Takenawa, T., Hwang, I., Fu, Y., and Yang, Z. (2010). Phosphoinositides regulate clathrin-dependent endocytosis at the tip of pollen tubes in *Arabidopsis* and tobacco. Plant Cell **22:** 4031–4044.